bioRxiv preprint doi: https://doi.org/10.1101/2021.09.01.458526; this version posted March 1, 2022. The copyright holder for this preprint (which was not certified by peer review) is the author/funder, who has granted bioRxiv a license to display the preprint in perpetuity. It is made available under aCC-BY 4.0 International license.

Tradeoff breaking as model of evolutionary transitions in individuality and the limits of the fitness decoupling metaphor

Pierrick Bourrat[1,2*], Guilhem Doulcier[1,5*], Caroline J. Rose[4], Paul B. Rainey[3,5], Katrin Hammerschmidt[6]

[1]Philosophy Department, Macquarie University, New South Wales 2109, Australia.

[2]Department of Philosophy & Charles Perkins Centre, The University of Sydney, New South Wales 2006, Australia.

[3]Laboratory of Biophysics and Evolution, Chemistry, Biology and Innovation (CBI) UMR8231, ESPCI Paris, CNRS, PSL Research University, 10 rue Vauquelin, Paris, France.

[4] Centre d'Écologie Fonctionnelle et Évolutive (CEFE), CNRS, Montpellier, France.

[5] Max Planck Institute for Evolutionary Biology, Plön, Germany.

[6] Institute of Microbiology, Kiel University, Kiel, Germany.

*These authors contributed equally to this work.

Author ORCIDs

Pierrick Bourrat https://orcid.org/0000-0002-4465-6015

Guilhem Doulcier https://orcid.org/0000-0003-3720-9089

Caroline J Rose https://orcid.org/0000-0001-7133-0355

Paul B Rainey https://orcid.org/0000-0003-0879-5795

Katrin Hammerschmidt https://orcid.org/0000-0003-0172-8995

Correspondence should be addressed to PB p.bourrat@gmail.com, GD guihem.doulcier@normalesup.org, and KH katrinhammerschmidt@googlemail.com.

Abstract

bioRxiv preprint doi: https://doi.org/10.1101/2021.09.01.458526; this version posted March 1, 2022. The copyright holder for this preprint (which was not certified by peer review) is the author/funder, who has granted bioRxiv a license to display the preprint in perpetuity. It is made available under aCC-BY 4.0 International license.

Evolutionary transitions in individuality (ETIs) involve the formation of Darwinian collectives from Darwinian particles. The transition from cells to multicellular life is a prime example. During an ETI, collectives become units of selection in their own right. However, the underlying processes are poorly understood. One observation used to identify the completion of an ETI is an increase in collective-level performance accompanied by a decrease in particle-level performance, for example measured by growth rate. This seemingly counterintuitive dynamic has been referred to as "fitness decoupling" and has been used to interpret both models and experimental data. Using a mathematical approach, we show this concept to be problematic in that the fitness of particles and collectives can never decouple—calculations of particle and collective fitness performed over appropriate and equivalent time intervals are necessarily the same. By way of solution, we draw attention to the value of mechanistic approaches that emphasise traits, and tradeoffs among traits, as opposed to fitness. This trait-based approach is sufficient to capture dynamics that underpin evolutionary transitions. In addition, drawing upon both experimental and theoretical studies, we show that while early stages of transitions might often involve tradeoffs among particle traits, later—and critical—stages are likely to involve the rupture of such tradeoffs. Thus, tradeoff-breaking stands as a useful marker for ETIs.

Keywords: Evolutionary transitions in individuality; Tradeoff; Evolutionary constraints; Fitness landscapes; Transfer of fitness; Export of fitness; Major transitions, Multicellularity; Life-history traits; Lande's equation; Lifecycle; Matrix population models; Division of labour; Ecological scaffolding; Mutation ratchet.

bioRxiv preprint doi: https://doi.org/10.1101/2021.09.01.458526; this version posted March 1, 2022. The copyright holder for this preprint (which was not certified by peer review) is the author/funder, who has granted bioRxiv a license to display the preprint in perpetuity. It is made available under aCC-BY 4.0 International license.

Introduction

Evolutionary transitions in individuality (ETIs) are events of major significance in the history of life. They begin with lower-level entities (particles) and complete when higher-level entities (collectives) acquire properties sufficient to participate directly in the process of evolution by natural selection (see Glossary for definitions of technical terms). ETIs of particular note include the evolution of chromosomes (from genes), the eukaryotic cell (from an ancestral eubacterium and archaebacterium) and multicellularity (from single cells) (Bouchard & Huneman, 2013; Bourke, 2011; Buss, 1987; Calcott & Sterelny, 2011; Jablonka, 1994; Maynard Smith & Szathmáry, 1995; Michod, 1999; van Gestel & Tarnita, 2017; West et al., 2015). Here, we focus attention on the transition from cells to multicellular life.

Evolutionary dynamics underpinning the transition to multicellularity have proven difficult to capture; however, influential for theory—and guiding experimental analysis—has been the concept of "fitness decoupling," which posits that the fitness of a collective in the early stage of a transition is directly proportional to the fitness of its particles and that, as the evolutionary transition proceeds, collective fitness "becomes decoupled from the fitness of its lower-level components" (Michod et al., 2003, p. 96). This notion is based on the fact that the evolution of cooperation, division of labour, or conflict-mediating mechanisms seem to improve collective-level fitness at the cost of particle-level fitness. This phenomenon has been interpreted through the lens of the export-of-fitness framework, in which the evolution of such mechanisms mark "transfer of fitness" from particle to collective levels (Michod et al., 2003; Michod, 2005; Okasha, 2006, 2009; Folse & Roughgarden, 2010).

While this theoretical model seems to be intuitive, and empirical tests straightforward, we demonstrate here that this is not the case. Not only is the notion of fitness and its use in evolutionary thinking generally problematic (as pointed out, among others, by Doebeli et al., 2017), but measurement of fitness in experiments—particularly in the context of ETIs, where fitness is usually compared between two organisational levels—is also difficult (Bourrat, 2015b, 2015a, 2021a). Experimental investigations of early stages in the transition to multicellularity (Hammerschmidt et al., 2014; Rose et al., 2020) are a good example thereof. Data from these experiments showed collective-level fitness to have improved while cell-level fitness declined over evolutionary time, giving the impression that the fitness of cells had decoupled from the fitness of collectives (see below for details). While several proxies for fitness were obtained, such as maximum growth rate and competitive fitness (as is traditionally done in the field, see Lenski et al., 1991; Wiser et al., 2013; Wiser & Lenski, 2015), for practical reasons it was impossible to measure cell and collective fitness over the same timescale, which would have been required for a meaningful comparison (see Box 1).

Building on this experimental approach and philosophical insights on the concept of fitness from Bourrat (2015a, 2015b), Black et al. (2020) constructed a simple "ecological scaffolding" model that showed how a minimal set of ecological conditions can produce evolutionary dynamics where particle and collective fitness appear

bioRxiv preprint doi: https://doi.org/10.1101/2021.09.01.458526; this version posted March 1, 2022. The copyright holder for this preprint (which was not certified by peer review) is the author/funder, who has granted bioRxiv a license to display the preprint in perpetuity. It is made available under aCC-BY 4.0 International license.

"decoupled". Population structure creates a tradeoff between short-term growth through particle division and long-term growth through collective persistence. This led Black et al. to conclude that a "fitness decoupling" observation can be explained in terms of a reduction of *short-term* particle growth rate coinciding with increased collective-level performance (over a *longer* timescale), rather than in terms of transfer of fitness between particles and collectives. We return to this point below and show formally that particle and collective fitness, when computed within the same reference environment (including timescale), cannot be decoupled under the assumption that collectives cannot grow indefinitely.

If it is true that the fitness of cells and collectives cannot decouple, where does this leave our understanding of dynamic processes that underpin ETIs? The mechanistic approach with an ecological focus is one route (see Black et al., 2020; Bourrat, in press; Doulcier et al., 2020), as is the ratcheting-mutation model proposed by Libby et al (2016). However, there is also a need to identify hallmarks of transitions that might allow identification and experimental validation of ETIs.

We begin by elaborating on the problem of "fitness decoupling," stressing that the problem, at its core, is not with the sense of complex dynamics expected to unfold when selection moves to operate over multiple timescales (or levels of organisation). Rather, it stems from the fact that the concept is tied to the currency of fitness (Section 1). In Section 2, we provide a population projection model of an abstract proto-multicellular organism and show how comparable measures of cell and collective fitness can be obtained, revealing the impossibility of fitness decoupling. In Section 3, we show that the intuited dynamics of transitions are captured best by the language of traits and tradeoffs among traits. Finally, we turn to the challenge of defining essential features of ETIs and argue that events that break the tradeoff constraining the ancestral particle — hereafter referred to as "tradeoff breaking"— stand as a general marker of ETIs (Sections 4 and 5).

Results

1. Challenges arising from application of fitness-centred approaches to the study of ETIs

One classical way to characterise particle fitness is to measure long-term reproductive success under a given set of environmental conditions relative to other particles (Pence & Ramsey, 2013; Doulcier et al., 2021). In a more practical sense, fitness is often measured as a per capita growth rate—that is, the average number of offspring produced by an individual per unit of time (or per generation) (Fisher, 1930; Metz et al., 1992). Whenever a nested system (composed of particles assembled into collectives) is studied, it is possible to measure at least two kinds of "fitnesses": the fitness of particles and that of collectives. To do so, population growth is tallied at each level.

Proponents of the export-of-fitness model and the concept of fitness decoupling argue that during an ETI, the fitness of particles and collectives of particles become "decoupled" (Michod & Roze, 1999; Michod et al., 2003; Michod, 2005; Shelton & Michod, 2010; Hanschen et al., 2015a, 2017; Shelton & Michod, 2020; Davison &

bioRxiv preprint doi: https://doi.org/10.1101/2021.09.01.458526; this version posted March 1, 2022. The copyright holder for this preprint (which was not certified by peer review) is the author/funder, who has granted bioRxiv a license to display the preprint in perpetuity. It is made available under aCC-BY 4.0 International license.

Michod, 2021). More precisely, the two values are predicted not to change in the same way and even to change in different directions: collective-level fitness increases while particle-level fitness decreases (Hanschen et al., 2017). Note that they are not expected to necessarily become independent from one another. All that is required for them to become decoupled is that they are anticorrelated or even less correlated. In some stricter formulations of the concept, collective and particle fitnesses are said to be decoupled as soon as collective fitness is not proportional to the average fitness of its component particles (Michod et al., 2003; Okasha, 2006). In this section, we review the theoretical and empirical arguments leading to this prediction.

The idea of fitness decoupling can be traced back to the study of the disruption of higher-level entities by the proliferation of lower-level entities composing them (see Maynard Smith & Szathmáry, 1995, pp. 7–8). If selection acts at two levels during an ETI, why would selection at the lower level (on molecules, cells, or organisms) not disrupt the effect of selection at the higher level (on chromosomes, multicellular organisms, or insect colonies)? Such "conflicts" pose a challenge for integration at the higher level. This phenomenon is present at all organismal levels. For instance, cancerous cells proliferating at a higher rate than healthy cells pose a threat to organismal integrity (Merlo et al., 2006). Similarly, without suppression from the queen, egg-laying worker bees pose a threat to the integrity of the hive (Amdam & Page, 2010). Other examples include selfish genetic elements, which can sometimes produce harmful effects at the organism level (see Werren, 2011 for a review). As a consequence, one may *prima facie* expect evolutionary trajectories to be the result of opposing processes that would be both a hallmark and a significant hurdle for ETIs.

The idea of fitness decoupling was introduced by Michod and Nedelcu (2003, pp. 66–67) to describe the ways conflicts between the higher and lower levels of organisation can be resolved during an ETI: "as the evolutionary transition proceeds, group fitness becomes decoupled from the fitness of its lower-level components [...] This transfer and reorganization of fitness components from lower to higher-levels occurs through the evolution of cooperation and mediators of conflict that restrict the opportunity for within-group change and enhance the opportunity for between-group change." More generally, Hanschen et al. (2017) note that "[a]ny trait that is costly at the lower level but beneficial at the group level enhances the fitness of the group at the expense of lower-level fitness and may therefore contribute to fitness decoupling and the emergence of indivisibility of the group." Okasha and Michod recast the notion of fitness decoupling in the multilevel selection 1 / multilevel selection 2 (MLS1/MLS2) framework (Michod, 2005; Michod & Nedelcu, 2003; Okasha, 2006, p. 232). Okasha, relying on Michod and colleagues' work, describes collective fitness during the three stages of an evolutionary transition (Okasha, 2006, p. 238): in the first stage, collective fitness is defined as average particle fitness (MLS1); second, collective fitness is defined as proportional to average particle fitness; finally, gradual decoupling occurs in the transition towards the third stage where collective fitness is no longer proportional to particle fitness (MLS2). In the export-of-fitness framework of ETIs, collectives initially 'lack' individuality (fitness of particles and collectives are proportional) and 'gain' individuality once their fitness is 'transferred' from the underlying particle (Michod & Roze, 1999; Okasha, 2006, pp. 234–235).

bioRxiv preprint doi: https://doi.org/10.1101/2021.09.01.458526; this version posted March 1, 2022. The copyright holder for this preprint (which was not certified by peer review) is the author/funder, who has granted bioRxiv a license to display the preprint in perpetuity. It is made available under aCC-BY 4.0 International license.

The concept of fitness decoupling has been regarded as one indicator for the ETI from cells to multicellular individuals (Rainey & Kerr, 2010; Pichugin, 2015; Hanschen et al., 2015b; Conlin et al., 2019). In a study using experimental bacterial (*Pseudomonas fluorescens*) populations, Hammerschmidt et al. (2014) and Rose et al. (2020) propagated collectives over multiple generations, and then asked whether predicted increases in collective-level fitness were realised. This was achieved by competing derived collectives against ancestral collectives over the timeframe of a single lifecycle generation—the number of offspring collectives left over this period was greater in the derived populations (Figure 1a). Next, they sought understanding of cell-level fitness effects. Ideally, such assays would have been performed over an entire collective-level life cycle; however, for practical reasons, this is nigh impossible. Instead, various cell-level assays were conducted, including assessment of competitive ability in broth culture. Data from these experiments showed cell-level fitness to have declined in derived populations (Figure 1b), at least for the regime where lineages passaged through soma-like and germ-like phases, giving the impression that the fitness of cells had decoupled from the fitness of collectives (Figure 1).

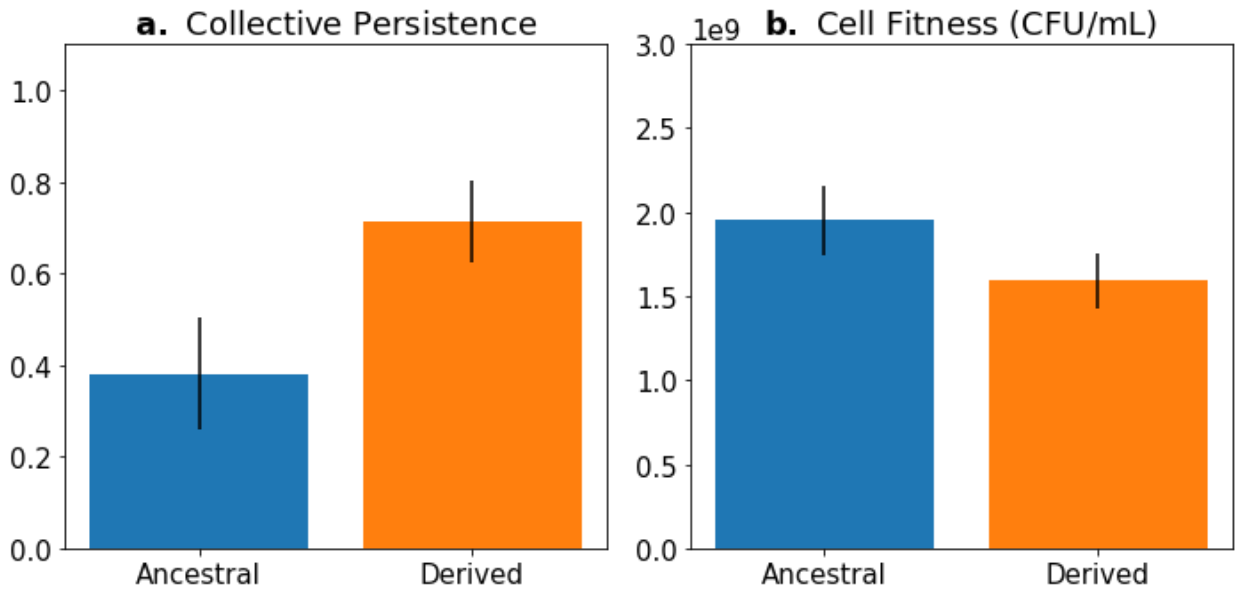

Figure 1 ***Fitness-decoupling observation in the Pseudomonas system.*** *Comparison of collective-level persistence (measured as the proportion of collective persistence after one generation when competed against an ancestral reference strain) and cell (particle) fitness (measured as the number of cells comprising a collective) for ancestral (blue) and derived (orange) populations under a regime designed to promote an ETI. Error bars represent standard errors of the mean (based on n=15 ancestral and n=14 derived lineages, respectively). Redrawn from Hammerschmidt et al. (2014, Fig. 2) for ease of comparison with Figure 5. Protocol described and statistical analysis performed in Hammerschmidt et al. (2014), showing statistical significance between ancestral and derived collective persistence/cell fitness. Dataset published as Rose et al. (2018).*

While fitness decoupling and the export-of-fitness model might seem useful concepts for understanding ETIs, we show formally here that commensurably computed fitnesses cannot generally be decoupled. Central to our argument (detailed in Section 2 and Box 1) is the need for measures of cell and collective fitness to derive from

bioRxiv preprint doi: https://doi.org/10.1101/2021.09.01.458526; this version posted March 1, 2022. The copyright holder for this preprint (which was not certified by peer review) is the author/funder, who has granted bioRxiv a license to display the preprint in perpetuity. It is made available under aCC-BY 4.0 International license.

analyses performed in the same reference environment and over precisely the same timescale (Black et al., 2020; Bourrat, 2015b, 2015a). In the example discussed above, collective fitness is computed by considering a full collective generation, while particle fitness is computed within collective development. This renders the comparison spurious, as illustrated in Figure 2. Computing the fitnesses at the same timescale and, thus, in the same reference environment would involve simultaneously tallying the increase of individual cells and number of collectives in a timeframe spanning several collective cycles.

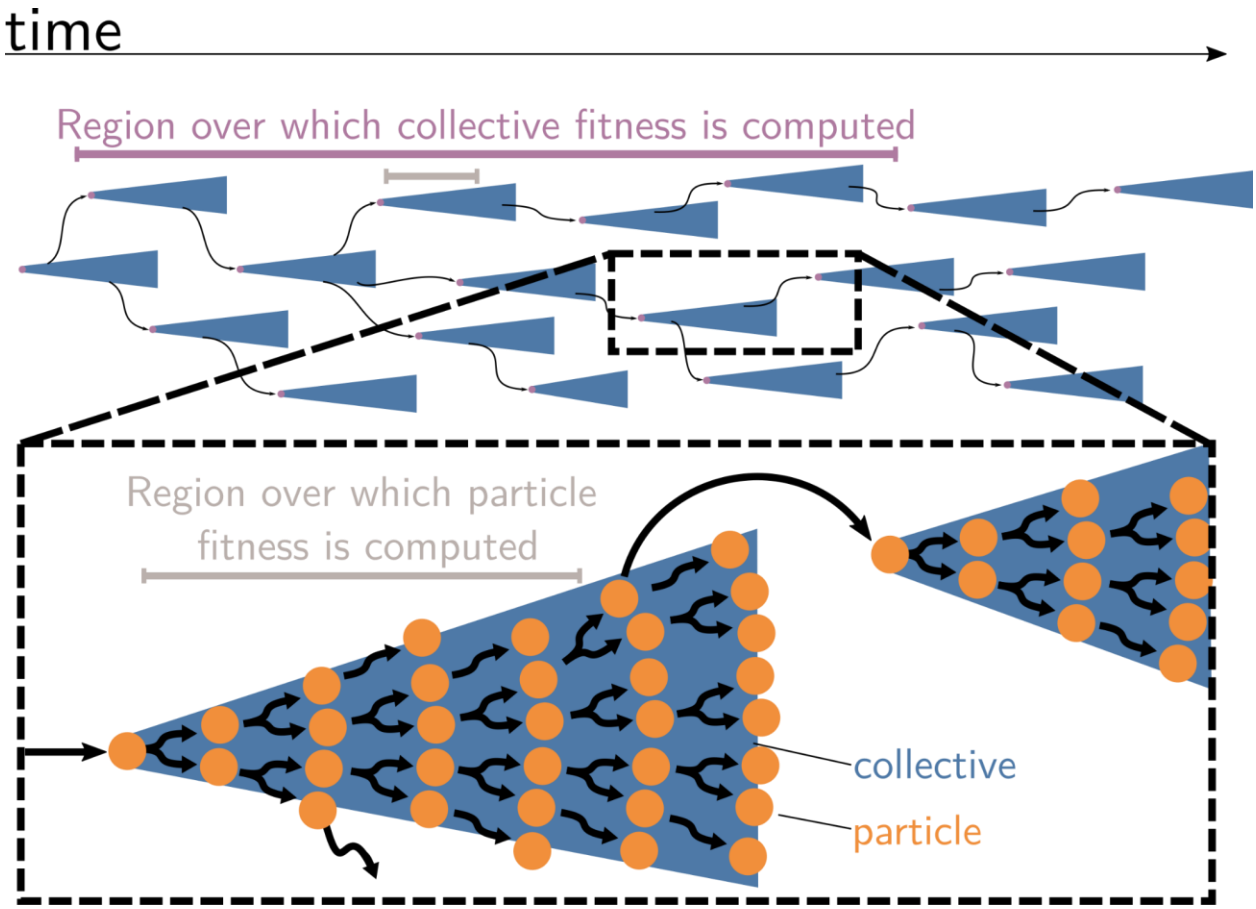

Figure 2 ***Collective and particle fitnesses are not measured over the same environment.*** *During an ETI, there are two levels of organisation: collectives (blue triangles) are composed of particles (orange disks). Both levels have their own genealogy (black arrows). Collective fitness is computed by considering one or several full collective generations (purple timeline), while particle fitness is computed within each collective development (grey timeline). As a result, they may exhibit opposing dynamics (increasing for collective and decreasing for particle fitness), giving rise to the fitness-decoupling observation.*

bioRxiv preprint doi: https://doi.org/10.1101/2021.09.01.458526; this version posted March 1, 2022. The copyright holder for this preprint (which was not certified by peer review) is the author/funder, who has granted bioRxiv a license to display the preprint in perpetuity. It is made available under aCC-BY 4.0 International license.

2. Commensurably computed particle and collective fitness are equal

In this section, we present a population projection model (Leslie, 1945; Caswell, 1989b) of an abstract proto-multicellular organism. The population is divided into classes corresponding to different sizes of collectives, as is commonly done in the literature (Tarnita et al., 2013; Pichugin et al., 2017). We define collective fitness in the context of this model (Section 2.2) and illustrate the different conventions that can be used to define particle fitness (Section 2.3). We provide proof that, under minimal conditions, if particle and collective fitness are computed with respect to the same set of events (i.e., in the same reference environment), they are equal (Section 2.3). Finally, we use this result to clarify conditions under which fitness-decoupling observations can be made (Section 2.4). Significantly, this model assumes that particles and collectives can coexist. In other words, we do not model the potential competition between particles and collectives as done in Tarnita et al. (2013). Also, we do not study the problem posed by the existence of free-riders or cheaters in collectives. However, this could be done by adding a game-theoretic layer to our model.

2.1 Modeling a nested demography

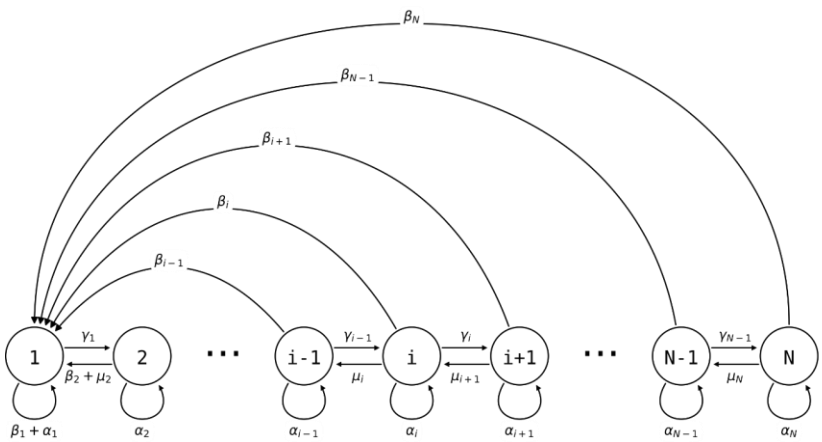

$$\mathbf{A} = \begin{pmatrix} \beta_1+\alpha_1 & \beta_2+\mu_2 & \cdots & \beta_{i-1} & \beta_i & \beta_{i+1} & \cdots & \beta_{N-1} & \beta_N \\ \gamma_1 & \alpha_2 & \cdots & 0 & 0 & 0 & \cdots & 0 & 0 \\ \vdots & \vdots & \ddots & \vdots & \vdots & \vdots & \ddots & \vdots & \vdots \\ 0 & 0 & \cdots & \alpha_{i-1} & \mu_i & 0 & \cdots & 0 & 0 \\ 0 & 0 & \cdots & \gamma_{i-1} & \alpha_i & \mu_{i+1} & \cdots & 0 & 0 \\ 0 & 0 & \cdots & 0 & \gamma_i & \alpha_{i+1} & \cdots & 0 & 0 \\ \vdots & \vdots & \ddots & \vdots & \vdots & \vdots & \ddots & \vdots & \vdots \\ 0 & 0 & \cdots & 0 & 0 & 0 & \cdots & \alpha_{N-1} & \mu_N \\ 0 & 0 & \cdots & 0 & 0 & 0 & \cdots & \gamma_{N-1} & \alpha_N \end{pmatrix}$$

Figure 3 ***Life cycle of collectives as a size–class population projection model.*** *Circles represent a size class of collectives; arrows represent the flow of individuals between size classes. At each time step, collectives of size class i can grow (if i<N), shrink or stay the same size. They also leave propagules of size class 1. See main text for details.*

Consider a population of genetically homogeneous *particles*, structured into *collectives* following the life cycle illustrated in Figure 3. Each collective is characterised by its size—that is, the number of particles it comprises. At each time step, a proportion γ_i of collectives of size class *i* increase to size class *i+1*, a proportion μ_i shrinks to size class *i-1,* a proportion δ_i dies, and the remaining collectives (i.e. a proportion $\alpha_i = 1 - \delta_i - \mu_i - \gamma_i$) stay the same size. Let N be the maximum size above which collectives cannot grow. Here, the collectives are voluntarily abstract because the statement the model supports is quite general, but one can consider that the particles are cells and growth and shrinkage of the collective is mediated by cell duplication and death. Additionally, collectives

bioRxiv preprint doi: https://doi.org/10.1101/2021.09.01.458526; this version posted March 1, 2022. The copyright holder for this preprint (which was not certified by peer review) is the author/funder, who has granted bioRxiv a license to display the preprint in perpetuity. It is made available under aCC-BY 4.0 International license.

reproduce: a collective of size *i* produces on average β_i propagules of size class 1 at each time step. Such a life cycle can be represented as a population projection model, whose dynamics are given by:

$$c_i(t+1) = \sum_{j=1}^{N} a_{ij} c_j(t),$$

where $c_i(t)$ is the density of collectives of size *i* at time *t,* and a_{ij} is the weight of the $i \rightarrow j$ edge of the life cycle graph (Figure 3; the a_{ij} are the elements of the population projection matrix **A**) for all values of *i* and *j* between *1* and *N*. It follows that the population density of particles is given by:

$$n(t) = \sum_{j=1}^{N} k_j c_j(t),$$

where *n(t)* is the number of particles within the population at time *t*, and k_j the number of particles corresponding to size class *j*. For instance, if we consider that all particles reproduce once for the collective to grow one size class, then $k_j = 2^{j-1}$.

2.2 Computing collective fitness

We define the fitness of collectives as the Malthusian parameter or asymptotic exponential growth rate of a population of collectives sharing the same trait value (Metz et al., 1992). If all transitions represented in the life cycle graph are possible, that is, $0 < \alpha_i < 1 \; \forall i = 1, 2, \ldots, N-1$, as well as $\beta_i > 0 \; \forall i = 1, 2, \ldots, N-1$, then the matrix $\mathbf{A} = (a_{ij})_{i,j \in [1,2 \ldots N]}$ is non-negative and primitive. Following the Perron-Frobenius theorem (see Caswell, 1989a, p. 57), there exists a positive eigenvalue of **A**, noted λ, called the dominant eigenvalue of **A** with an associated non-negative eigenvector **w**. Moreover, the strong ergodic theorem (see Caswell, 1989a, p. 57) shows that the long-term dynamics of the population are described by a growth rate λ and a stable population structure **w**. When these assumptions are met, the fitness of collectives is given by:

$$F = \lim_{t \to \infty} \left(\frac{ln\left(\sum_{j=1}^{N} c_j(t)\right) - ln\left(\sum_{j=1}^{N} c_j(0)\right)}{t} \right) = ln(\lambda). \qquad \text{(Eq. 1)}$$

where the first equality is given by the definition of fitness, the second by the Perron-Frobenius and strong ergodic theorems, and $c_j(t)$ is the density of collectives of size class *j* at time *t*.

bioRxiv preprint doi: https://doi.org/10.1101/2021.09.01.458526; this version posted March 1, 2022. The copyright holder for this preprint (which was not certified by peer review) is the author/funder, who has granted bioRxiv a license to display the preprint in perpetuity. It is made available under aCC-BY 4.0 International license.

2.3 Computing particle fitness

In contrast to collective fitness, computing particle fitness is more challenging. There are, *prima facie*, at least three ways to compute the fitness of a particle. Each gives rise to a different measure that we will call f_1, f_2 and f_3 (illustrated in Figure 4, their expression for the current model will be given later). To compute:

- f_1, look within each collective and consider the dynamics of the particles. This is equivalent to ignoring all the "between collective" level events (collective births and deaths). This is what is done experimentally when measuring cell density within isolated collectives (Figure 1, Hammerschmidt et al., 2014).
- f_2, look at a theoretical mono-particle collective. This is equivalent to ignoring all the "within collective" events (collective growth and shrinking). This conception of fitness corresponds to the notion of "counterfactual fitness" proposed by Shelton & Michod (2014, 2020) because it is equivalent to the fitness that particles *would* have if they were genetically equivalent (same trait values), but without the ability to produce multi-particle collectives. This is also close to the experimental measurements of cell density performed experimentally (Hammerschmidt et al., 2014, "growth rate" in ED Fig. 4) under conditions preventing the formation of collectives (shaking).
- f_3, take into account all events (i.e., within and between collective), with counts of the number of particles through time.

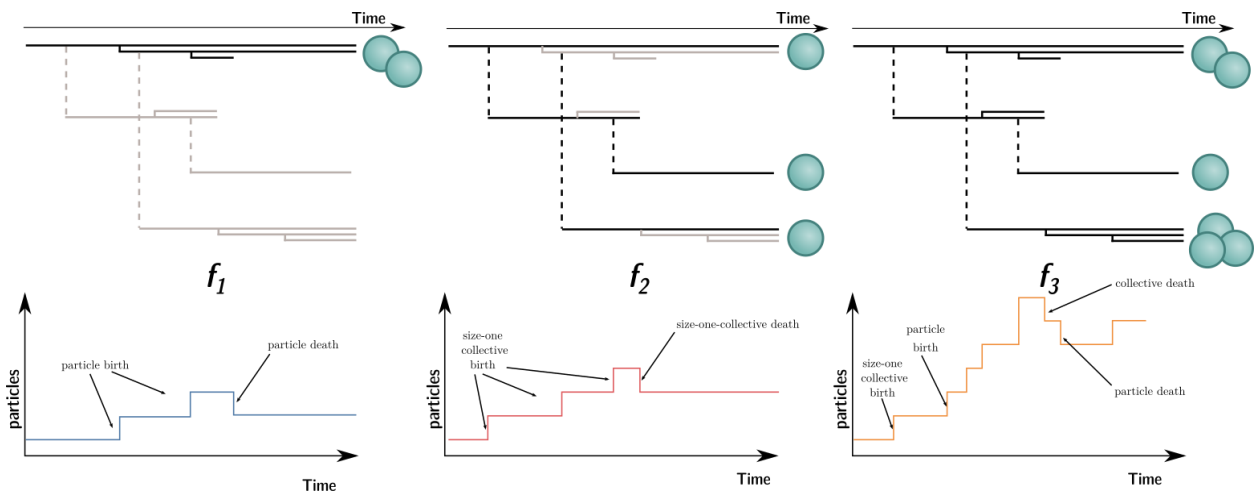

Figure 4 ***Three ways to compute particle fitness (f_1, f_2, and f_3) in a lineage starting from a single particle.*** *Top: Each solid horizontal line represents the lifespan of a particle. The vertical axis has no unit and only represents population structure. Particles within the same collectives are represented as a series of horizontal lines close to one another (isolated particles count as mono-particle collectives). Each dashed vertical line connects a parental collective to its offspring (which starts as a single cell). Greyed-out elements for f_1 and f_2 indicate the processes that are omitted during the fitness calculation. Bottom: the timeseries below each example shows how particles are tallied. In the case of f_1, between-collective events are ignored. Thus, the two particles are the only ones relevant for its computation, whereas in the case of f_2 within-collective birth–deaths and their effects are ignored. Thus, the three particles (i.e., mono-particle*

bioRxiv preprint doi: https://doi.org/10.1101/2021.09.01.458526; this version posted March 1, 2022. The copyright holder for this preprint (which was not certified by peer review) is the author/funder, who has granted bioRxiv a license to display the preprint in perpetuity. It is made available under aCC-BY 4.0 International license.

collectives) are relevant for its computation. Finally, in the case of f_3, the full lineage is used . Thus, all 6 particles must be taken into account for its computation.

Each of these ways to compute fitness uses a different reference environment (including the timescale). Each can be adequate in different contexts. It is appropriate to measure particle fitness considering within-collective events (f_1) only when the evolutionary process studied occurs in the short term. For instance, computing f_1 can tell us which mutant cell lineage can take over within an organism (e.g., cancerous lineages). The counterfactual method f_2 gives information on a "what if" world where particles cannot be organised in collectives (i.e., in the model, collectives cannot grow:$\gamma_i = 0$). It might give information on the unicellular ancestor of a collective. Indeed, a reasonable hypothesis is that the ancestral trait values are those that maximise counterfactual fitness (Shelton & Michod, 2020, p. 8).

However, there is no *a priori* reason for the values of f_1, f_2, and f_3 to be equal to each other, or even to change in the same direction when the traits of the organism change. This is clear in view of their expression in the model. Considering within-collective dynamics (ignoring the effect of density dependence, as is usually done in experiments) gives $f_1 = \ln(1 - \mu_1 + (k_2 - 1)\gamma_1)$.[1] In contrast, considering the counterfactual collective dynamics gives $f_2 = \ln(1 - \delta_1 + \beta_1)$. Comparing the two equations, we can see that f_2 does not depend on γ . It follows that an increase in γ would result in an increase in f_1 with no consequence on f_2. *Mutatis mutandis* the same applies for μ, δ and β.

The case of f_3 is different. The expression of f_3 is given by the long-term exponential growth rate of *n*, which is a linear combination of exponentially growing terms $k_i c_i(t)$ and, thus, asymptotically grows at the rate of its largest coefficient. By definition, this coefficient is λ , the dominant eigenvalue of **A**. Intuitively, this means that once the population has reached a stable size distribution, the relative proportion of different collective sizes do not matter for computing the overall growth rate of particles—they grow at the same rate as the collective population. Thus, $f_3 = \ln(\lambda) = F$. It follows that a change in γ (or μ, δ and β) would affect f_3 and F in the same way. This shows that when the particle fitness is computed with the same frame of reference (i.e., the same environment) as collective fitness (using the same timescale and the same set of events), the values are (mathematically) equal.

2.4 Fitness-decoupling observations do little to clarify the process of an ETI

With these distinctions in place and the constraint that, to be compared, fitnesses must be measured over the same set of events (i.e., same environment over the same timescale) (see Box 1 and Section 1), the apparent contradiction of a simultaneous increase in collective fitness and decrease in particle fitness of a single biological entity is dissolved. More precisely, either fitness at the particle and the collective level are commensurably computed—

[1] That is, the expected exponential growth rate of a discrete-time branching process (or Bienaymé-Galton-Watson process) where each individual leaves either 0, 1, or k_2 offspring with probabilities mu, $(1-\mu_1)(1-g_1)$, and $(1-\mu_1)g_1$, respectively.

bioRxiv preprint doi: https://doi.org/10.1101/2021.09.01.458526; this version posted March 1, 2022. The copyright holder for this preprint (which was not certified by peer review) is the author/funder, who has granted bioRxiv a license to display the preprint in perpetuity. It is made available under aCC-BY 4.0 International license.

that is, with respect to the same biological object and in the same reference environment—in which case they are equal (F and f_3), or they refer to different biological settings (f_1 or f_2 and F) and, thus, the biological significance of their differential dynamics is not immediately clear. Note that this result requires that the population reaches a stable size distribution; only if the collectives are able to grow (or shrink) indefinitely, which is not a realistic assumption for ETIs, could genuine fitness decoupling be observed (see Bourrat, 2021b, Chapter 5 for details) .

Consequently, the observation that F increases while f_1 or f_2 decreases through time does little on its own to clarify the process of an ETI because they are not commensurable. However, such fitness-decoupling observations can be understood as a consequence of an underlying tradeoff. In Section 5, we return to a biological scenario where fitness-decoupling observations would not be made. In the next section, we introduce a model of such a tradeoff that provides a plausible biological mechanism for the emergence of multicellular collectives under given conditions while displaying a simultaneous increase in F and a decrease in f_2 .

3. Tradeoffs between particle traits drive ETIs

The previous section showed that if collective and particle fitness are computed in the same reference environment, they are necessarily equal. In addition, it showed that a fitness-decoupling observation (e.g., f_2 and F going in different directions) offers little information about the mechanism of ETIs on its own since there is no reason to relate the dynamics of f_1 or f_2 to the one of collective fitness F without additional assumptions about the system (i.e., that ancestral particles and particles within the collective are restricted to the same subset of the trait space, e.g., by a tradeoff). In this section, we present an evolutionary model of ETIs that includes these additional assumptions (Section 3.1), describe under which conditions fitness-decoupling observations can occur (Section 3.2), and provide an example involving a tradeoff between two traits: the survival of existing collectives and the production of new cells (Section 3.3). This example features an increase of F and a decrease of f_2 along the evolutionary trajectory. We focus on f_2 because it is more relevant to ETIs; while f_1 has been discussed more strictly in the levels of selection literature, f_2 can be interpreted as the hypothetical fitness an ancestor cell would have (Shelton & Michod, 2020). Nonetheless, the same argument could be made for f_1.

3.1 Modeling evolution

The demographic model of Section 2 is completed with a model of evolution in two steps. First, consider that the life cycle of collectives (summarised by the population projection matrix **A**) depends upon a trait $\theta \in [0, 1]$ whose value can change by mutation. For each trait value θ, a corresponding fitness value $F(\theta)$ exists. Second, we use the simplifying assumptions of Lande's Equation (Caswell, 1989a, p. 164), namely the separation of demographic and evolutionary timescales, and the absence of density-dependent effects, and perform a successive invasion analysis. These assumptions lead to the following equation for the evolution of the average trait value $\bar{p}$ in the population:

bioRxiv preprint doi: https://doi.org/10.1101/2021.09.01.458526; this version posted March 1, 2022. The copyright holder for this preprint (which was not certified by peer review) is the author/funder, who has granted bioRxiv a license to display the preprint in perpetuity. It is made available under aCC-BY 4.0 International license.

$$\frac{d\overline{\theta}}{dt} = \sigma F(\overline{\theta})^{-1} \frac{dF}{d\theta}(\theta = \overline{\theta}) \quad \text{(Eq. 2)},$$

where $\sigma_\theta \in \mathbb{R}_+$ is the variance of mutation effects on the trait θ. As a consequence, the model predicts that the average value of the trait $\overline{\theta}$ will "climb up" the fitness gradient $\frac{dF}{d\theta}$ as fitter mutants emerge and invade the population.

The ancestral phenotype (i.e., the initial condition $\overline{\theta}(t=0)$ of the evolutionary trajectory) will be taken to be θ_0, the optimal trait value for the ancestral unicellular organism. Thus, $\theta_0 = \arg\max_\theta f_2(\theta)$, where $f_2(\theta)$ is the value of f_2 for an organism with trait θ. Similarly, let θ^* be the optimal trait value for the collective, where $\theta^* = \arg\max_\theta F(\theta)$. The code implementing this model and drawing the figures presented here is available as supplementary material (doi: 10.5281/zenodo.5352208). It uses the Matpopmod library (Bienvenu & Doulcier, 2021).

3.2 Conditions for fitness-decoupling observations between f_1 or f_2 and F

Once a mutation (or change in the environment) makes the first multi-particle collective possible, the process that drives population dynamics is one associated with F. A sufficient condition for fitness-decoupling observations to be possible would be that the trait values that are optimal for single-particle collectives (θ_0) are not optimal for multi-particle collectives ($\theta^* \neq \theta_0$), provided the fitness landscape is smooth enough (and both F and f_2 are continuous functions of θ with a single maximum value). Thus, as selection acts during the ETI and drives the trait values towards fitter collectives (towards θ^* the optimal value for F), this would necessarily lead to less fit "counterfactual" single-particle collectives (away from θ_0, the optimal value for f_2). Conversely, a sufficient condition to observe "coupling" between f_2 and f_3 (or F) would be that the optimal trait values for these two measures coincide ($\theta^* = \theta_0$) and that the ancestral trait was not optimal. Then, the evolutionary trajectory of the population would tend towards traits with a higher value of F and, coincidently, towards higher values of f_2 (hence the existence of a "coupling").

3.3 An example: The tradeoff between collective growth and persistence

Let $\theta \in [0,1]$ be a trait that controls the relative investment of the particles towards collective survival and collective growth modeled by parameters s and b such that $s = \theta$ and $b = 1 - \theta$. More precisely, let the probability for a collective of size class i to survive a single time step be p_i, with $p_1 \in [0,1]$ and for $i = 2, \ldots, N$, $p_i = 1 - e^{-\eta s}$ (where η is a scaling factor). Let the probability for a collective of size class i to grow to the next class size during a time step be g_i, with $g_i = 1 - e^{-\eta b}$ for $i = 1, \ldots, N-1$ and $g_N = 0$. Additionally, let the expected number of propagules shed by a collective of class size i be $m_i = \eta b k_i$. Thus, following the Birth-

bioRxiv preprint doi: https://doi.org/10.1101/2021.09.01.458526; this version posted March 1, 2022. The copyright holder for this preprint (which was not certified by peer review) is the author/funder, who has granted bioRxiv a license to display the preprint in perpetuity. It is made available under aCC-BY 4.0 International license.

Flow Class structured model (Caswell, 1989, pp. 83–93), the matrix projection model from Figure 3 is parameterised as such: $\alpha_i = p_i(1-g_i)$, $\gamma_i = p_i g_i$, and $\beta_i = p_1^{0.5}\frac{1}{2}((1+\alpha_i)m_i + \gamma_i m_{i+1})$. For this example, consider that collectives cannot shrink by setting $\mu_i = 0$.

In this model, the optimal trait value for counterfactual (f_2) fitness is always a null investment in collective survival $\theta = 0$. However, the optimal trait value for whole life cycle fitness (*F*) is $\theta > 0$. Thus, if a population starts with the optimal trait value for the counterfactual fitness $\theta_0 = 0$, it will evolve towards the optimal value $\theta^* > 0$ (green arrow, Figure 5). Over time, collective-level fitness *F* increases while counterfactual fitness f_2 decreases.

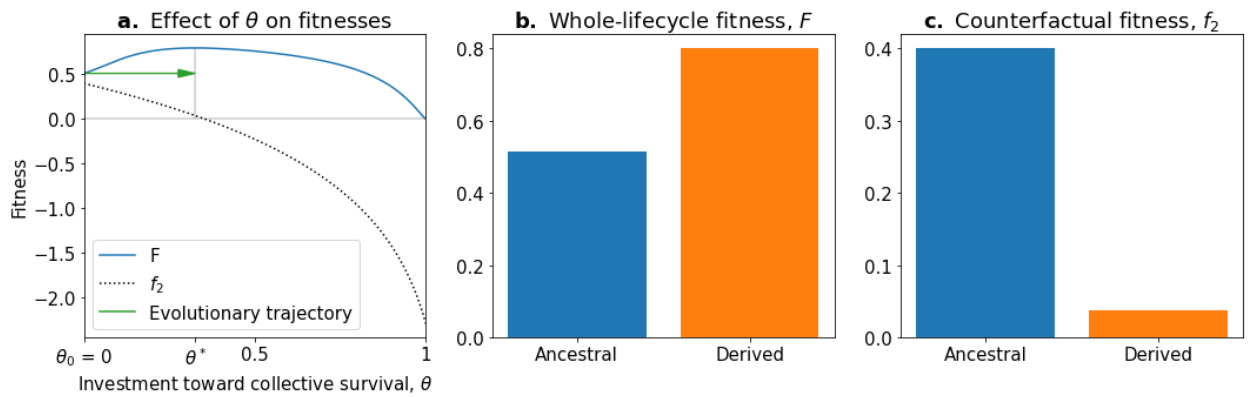

Figure 5 ***The tradeoff model can reproduce the fitness-decoupling observation. a.*** *Values of F and f_2 as a function of the trait θ.* ***b.*** *Ancestral and derived values of whole–lifecycle fitness (F).* ***c.*** *Ancestral and derived values of counterfactual fitness (f_2). The expected evolutionary trajectory from ancestral (θ_0) to derived (θ^*) trait value (green arrow in a.) results in an increase of F and a decrease of f_2 reproducing the fitness-decoupling observation of Figure 1. Parameters: $N = 30$, $\eta = 8$, and $p_1 = 0.1$.*

This evolution towards higher values of θ (because it increases *F*) coinciding with a decrease in f_2 leads to a fitness-decoupling observation. Note, importantly, that following the assumptions of the model, the opposite directions of the dynamics of *F* and f_2 are a consequence of optimal trait values on a tradeoff being different in different environments, not an inherent relationship between them. To see this, consider the example of selection on settlement in *Saccharomyces cerevisiae* (Ratcliff et al., 2012). The optimal trait value for an ancestral particle (i.e., a free living cell) is having round cells. However, in a snowflake aggregate, the optimal shape is to be elongated because this shape permits packing of more cells. In this example, f_2 decreases—to be elongated in the ancestral environment would be disadvantageous—when whole–life cycle fitness *F* increases: to be elongated is advantageous in the context of the snowflake. We see here that the relative changes in fitness F and f_2 do not explain the dynamics observed but rather follow from changes in environmental conditions and genetic and phenotypic constraints on cells. In the next section, we propose instead that one genuine marker for an ETI is the capacity for a lineage to break away from such a tradeoff. Patterns of tradeoff-breaking correspond with the

bioRxiv preprint doi: https://doi.org/10.1101/2021.09.01.458526; this version posted March 1, 2022. The copyright holder for this preprint (which was not certified by peer review) is the author/funder, who has granted bioRxiv a license to display the preprint in perpetuity. It is made available under aCC-BY 4.0 International license.

emergence of novel collective-level traits—that is, traits that can only be exhibited in a collective context—and, as such, provide an evolutionary cause of ETIs.

4. Tradeoff-breaking as markers of ETIs

In the previous section, we saw that a tradeoff between traits can result, under specific conditions, in an empirical fitness-decoupling observation. Evolutionary tradeoffs between traits are a consequence of the genetic background of organisms and their environment. Thus, they are not immutable and can evolve if some changes in the genetic background or the environment occur. In this section, we propose that a marker of an ETI is "breaking" from the initial tradeoff (hereafter called "tradeoff-breaking" observations'). To explain this phenomenon, we present a modification to the model described in Section 3, which we call the "tradeoff-breaking model".

A tradeoff is essentially a constraint on the combined values of a set of traits; it prevents a given organism from simultaneously performing well in two or more functions: for instance, growth and survival or photosynthesis and nitrogenase activity in cyanobacteria, as discussed below. Thus, if a mutant lineage is able to bypass the tradeoff and perform well in different functions, it is expected to be fitter than its ancestor and increase in proportion in the population. In some cases, mutations that lead to a multicellular morphology might be a necessary step towards bypassing or breaking the tradeoff. This provides an "adaptive" explanation for the emergence of multicellular organisms. Collectives (i.e., multicells) emerge by mutations constrained by the tradeoff, but their long-term persistence is rendered more probable by tradeoff-breaking mutations that would not have been possible, or would not have broken the tradeoff, had they occured in their unicellular ancestors.

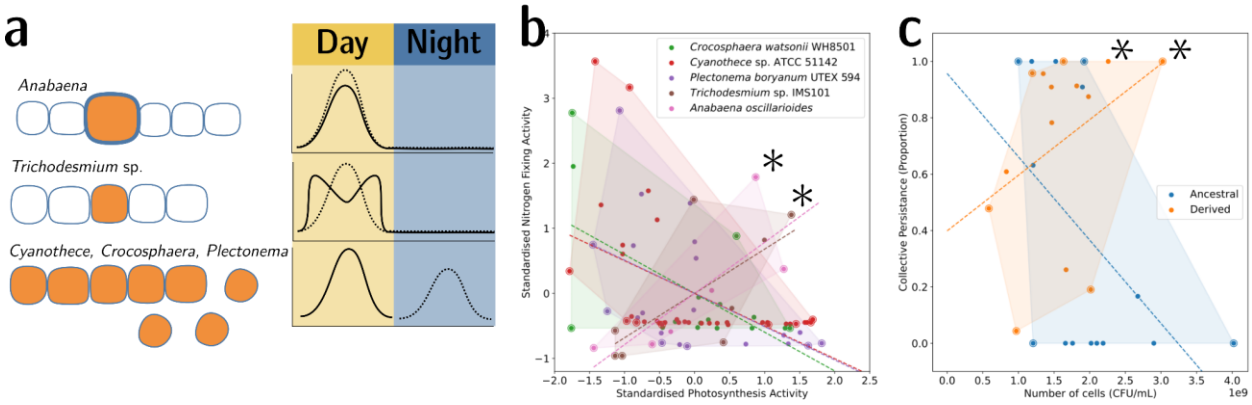

Figure 6 ***Tradeoff-breaking lineages can be inferred experimentally. a.*** *Morphological and physiological N_2-fixing adaptations for different cyanobacteria. Orange shaded areas indicate nitrogenase localisation. Daily rhythm of photosynthesis (solid line) and N_2-fixation (dashed line) (modified from Berman-Frank et al., 2003).* ***b.*** *Tradeoff between photosynthesis activity and nitrogenase activity in cyanobacteria (data taken from Colon-Lopez et al., 1997; Mohr et al., 2013; Misra & Tuli, 2000; Berman-Frank et al., 2001; Popa et al., 2007 and standardised). The shaded area for a given species corresponds to the convex hull of observations. Assuming a representative*

bioRxiv preprint doi: https://doi.org/10.1101/2021.09.01.458526; this version posted March 1, 2022. The copyright holder for this preprint (which was not certified by peer review) is the author/funder, who has granted bioRxiv a license to display the preprint in perpetuity. It is made available under aCC-BY 4.0 International license.

sampling, it stands for the expected range of traits accessible for this species. Dashed lines are least-square linear regressions of the observations of each species; asterisks indicate potential tradeoff-breaking observations because they notably depart from the tradeoff pattern displayed by most species. ***c.*** *Tradeoff between collective persistence and cell number in Pseudomonas fluorescens for ancestral and derived lineages (Hammerschmidt et al., 2014, asterisks indicate tradeoff-breaking observations in two lineages). Dataset published as Rose et al. (2018).*

To illustrate this point, we provide two examples from biology. The first one is the well-understood tradeoff between photosynthesis and nitrogen fixation—from dinitrogen gas (N_2)—in cyanobacteria. The tradeoff is caused by the oxygen sensitivity of the enzyme nitrogenase, which catalyses the process of reducing N_2 to ammonia (NH_3). This prevents cells from performing both functions simultaneously and has resulted in several morphological and physiological adaptations (Figure 6a). In the unicellular species, *Cyanothece* sp. ATCC 51142 and *Crocosphaera watsonii* WH8501, and the undifferentiated filamentous *Plectonema boryanum* UTEX 594, the two functions are temporally separated by a circadian rhythm: the oxygen-sensitive N_2 fixation is performed during the night, unhindered by the oxygen-producing photosynthesis during the day. When plotting the activity values for photosynthesis and N_2 fixation for populations of these species, they fall on both sides of the tradeoff—depending on the time of the day (Figure 6b). In the morphologically undifferentiated filamentous multicellular *Trichodesmium* sp. IMS101, the two functions are performed simultaneously, but in different, morphologically identical cells of the filament. Thus, the values for these populations are located in the middle of the tradeoff—they perform averagely in both functions. This pattern can also be seen for populations of the highly differentiated filamentous *Anabaena oscillarioides*, which perform even better than the undifferentiated *Trichodesmium* sp.. This can be explained by the presence of differentiated cells (heterocysts) that only fix N_2 and exchange the fixed nitrogen compounds against carbon products with the photosynthesising cells of the filament. This example seems to be compatible with the tradeoff-breaking framework—both multicellular and (physiologically) differentiated species, *A. oscillarioides* and *Trichodesmium* sp., seem to have broken away from the tradeoff, which leads to tradeoff-breaking observations in Figure 6b (indicated by asterisks). Moreover, photosynthesis and nitrogen fixation are positively associated, as indicated by the regression line. Overall, the example of cyanobacteria illustrates how tradeoff-breaking can occur—multicellular differentiated morphology and designated N_2-fixing cells allow the organisms to break away from the tradeoff that is present in the unicellular and physiologically undifferentiated phyla (visible in Figure 6b as the three negative regression lines).

The second example is the derived *Pseudomonas fluorescens* populations, where tradeoff-breaking seems to have occurred in some of the evolved lineages. In this case, the tradeoff implies that collective persistence cannot increase concomitantly with cell number. However, in the experiment of Hammerschmidt et al. (2014), two lineages have succeeded in doing this, leading to two tradeoff-breaking observations visible in Figure 6c (indicated by asterisks). Here, collective persistence increased due to the evolution of a *mutS*-dependent genetic switch that enabled rapid and predictable transitioning between two stages of a life cycle. This increase in collective persistence is not accompanied by a decrease in cell density, as is the case in other lineages, indicative of these two lineages having broken the tradeoff.

bioRxiv preprint doi: https://doi.org/10.1101/2021.09.01.458526; this version posted March 1, 2022. The copyright holder for this preprint (which was not certified by peer review) is the author/funder, who has granted bioRxiv a license to display the preprint in perpetuity. It is made available under aCC-BY 4.0 International license.

The model presented in Section 3 cannot account for such changes affecting the traits, for example through mutations. To do so, it must be modified into what we refer to as the tradeoff-breaking model. In the model presented in Section 3, the traits survival *s* and growth *b* were linked by a deterministic relation through the investment trait *p*: $s = p$ and $b = 1 - p$. Thus, any mutation affecting one trait necessarily leads to opposite effects on the other. This assumption can be relaxed, allowing the two traits to take any pair of values. To keep modelling the tradeoff, we suppose that the distribution of mutational effects (the mutation kernel) is a two-dimensional Gaussian distribution with a high (negative) correlation value ($\rho = -0.9$). This means that most mutations that increase one trait value reduce the other. However, and this is crucial, some rare mutations have the effect of increasing or decreasing both values, something that was impossible in the model described in Section 3. Thus, Eq. 2 becomes:

$$\frac{d}{dt}\begin{pmatrix} s \\ b \end{pmatrix} = F(s,b)^{-1}\begin{pmatrix} \sigma_s^2 & \sigma_s\sigma_b\rho \\ \sigma_s\sigma_b\rho & \sigma_b^2 \end{pmatrix}\nabla F(s,b) \quad \text{(Eq 3)},$$

where $F(s,b)$ is the whole–life cycle fitness as a function of the traits, $\nabla F(s,b)$ is the fitness gradient in the two-dimensional trait space, and σ_s and σ_b are the variance of mutational effects on *s* and *b*, respectively. Figure 7 shows the trajectory resulting from this model. Initially, the population moves along the tradeoff in the trait-space: reducing the value of *b* and increasing the value of *s*. This reflects how "low hanging fruit" mutations—mutations that are more frequent due to the skew in the mutational effect distribution—drive the initial dynamics. This fast-paced phase of the dynamics (which can be absent in some cases; see next section) following a phase during which collectives are formed ends when the population reaches the neighbourhood of the optimal organism that lies on the tradeoff line *s = (1-b)* (around t_1). Then, a slower phase of the dynamics starts and leads to a tradeoff-breaking observation (the population "breaks away" from the tradeoff line; Figure 7a after t_1). This third phase is slower because mutations that move collectives in this direction are statistically less likely to occur. Figure 7b shows that observation of fitness decoupling between f_2 and *F* could only be made in the first part of the trajectory. However, the whole trajectory is characterised by an increase in fitness *F*, as discussed in Section 3.

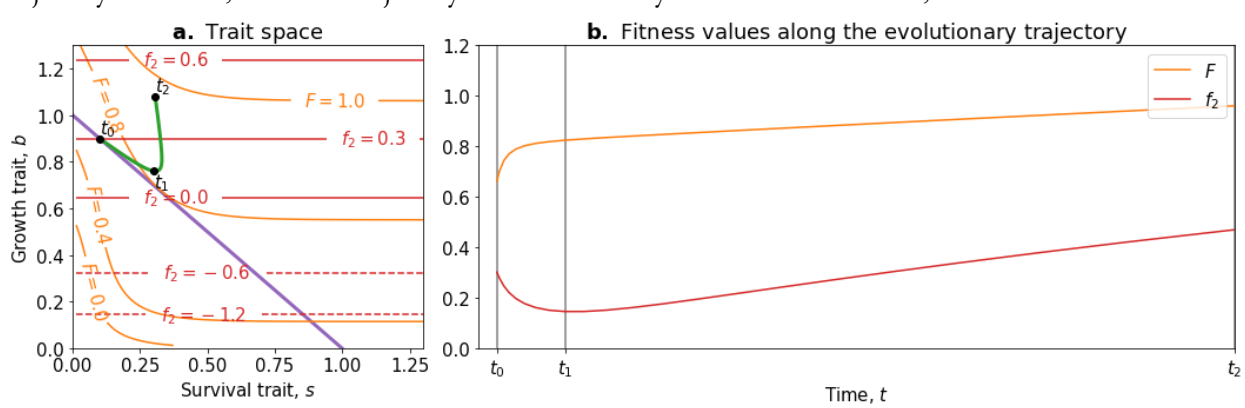

Figure 7 ***Tradeoff-breaking mutations do not fit the fitness-decoupling observation. a****. Trait space with isolines of fitness. An example of a possible evolutionary trajectory is shown in green.* ***b****. Particle (counterfactual; f_2 in red) and collective fitness (F in orange) values along the example evolutionary trajectory (in green). The strict tradeoff from Section 3 and Figure 5 is shown in purple. The times marked by vertical lines in* ***b*** *correspond to the dots in* ***a****. The evolutionary trajectory can be separated into two phases once collectives have been formed: a fast-paced phase (before t_1) that closely follows the purple tradeoff in* ***a****, and a slower phase (after t_1) that breaks away from it*

bioRxiv preprint doi: https://doi.org/10.1101/2021.09.01.458526; this version posted March 1, 2022. The copyright holder for this preprint (which was not certified by peer review) is the author/funder, who has granted bioRxiv a license to display the preprint in perpetuity. It is made available under aCC-BY 4.0 International license.

*and leads to the tradeoff-breaking observation. Note that a fitness-decoupling observation can only be made in the fast-paced phase of the trajectory (before t_1), as represented in **b**. Parameters: N=15,* $p_1 = 0.1, \eta = 8, \rho = -0.9$.

Our model gives a simple mechanism that can reproduce the experimental fitness-decoupling observation, in addition to the tradeoff-breaking observations due to rare mutants. Specifically, we observe that the trajectory resulting from the model is mirrored by the trajectory of lineages in the evolved *Pseudomonas fluorescens* populations (Hammerschmidt et al., 2014). When compared to the ancestral lineages, most of the evolved lineages appear to have been constrained by the tradeoff and increased in collective persistence at the expense of cell density (through low-hanging fruit mutations, as is the case between t_0 and t_1 in Figure 7). Notably, only the two outlier lineages (marked by asterisks in Figure 6c) seem to have started to break away from the tradeoff—they seem to have reached the slower phase of the evolutionary dynamic (where less likely mutations are explored, as is the case between t_1 and t_2 in Figure 7). Tentatively, the fact that only the two outlier lineages broke away from the tradeoff might be due to a higher mutation rate increasing the relative speed of evolution compared to the other lines. According to our tradeoff-breaking framework, the fitness-decoupling observation should be reinterpreted as lineages being in the fast-paced phase of the trajectory. Moreover, the tradeoff-breaking lineages should be explored (as done to an extent in Hammerschmidt et al., 2014) as we advocate that tradeoff-breaking observations are the mark of significant genetic innovation and, thus, can be used as a hallmark of ETIs.

The tradeoff-breaking model presented here is compatible with a number of different models of ETIs recently proposed in the literature. Among them are two models we think could benefit from being seen through the framework we developed here because they illustrate a diversity of mechanisms that yield initial tradeoffs and tradeoff-breaking mutations: the ratcheting model proposed by Libby and collaborators (Libby et al., 2016; Libby & Ratcliff, 2014) and the ecological scaffolding model proposed by Black et al. (2020). Further, recasting these two models in terms of tradeoff-breaking yields new insights, which are detailed in Boxes 2 and 3, respectively.

In the ratcheting model, proto-multicellular organisms are in an environment alternating between multicellular-favouring and unicell-favouring. This yields a tradeoff between the two states and the selection for a high probability of multicells to revert to unicells. Some mutations ("ratcheting (type 1) mutations") are assumed to be beneficial in a collective (multicellular) environment while deleterious in a unicellular context; thus, they play the tradeoff-breaking role. Libby et al. (2016) showed, through simulations, that the accumulation of ratcheting mutations makes it harder for a multicellular organism to revert to a unicellular state even when the environment becomes favourable for unicellularity.

In the ecological scaffolding model, the environment, structured both spatially and temporally, allows for selection of collective-level properties without need to assume anything about the particles other than that they reproduce at different rates. Black et al. (2020) showed that the tradeoff stems from population structure: reductions in cell growth rate are favoured due to benefits to collectives that are realised via improvements in

bioRxiv preprint doi: https://doi.org/10.1101/2021.09.01.458526; this version posted March 1, 2022. The copyright holder for this preprint (which was not certified by peer review) is the author/funder, who has granted bioRxiv a license to display the preprint in perpetuity. It is made available under aCC-BY 4.0 International license.

dispersal. The emergence of specialised soma cells is an example of tradeoff-breaking: it allows an increase in collective dispersal without requiring as much cell growth reduction.

Both models illustrate the flexibility of our tradeoff and tradeoff-breaking approach. First, it allows multiple mechanisms of evolutionary transitions to be formalised in a unified way. Second, tradeoff-breaking observations can be used as a general marker across various mechanisms of evolutionary transitions.

5. The trait-based approach in the context of ETIs

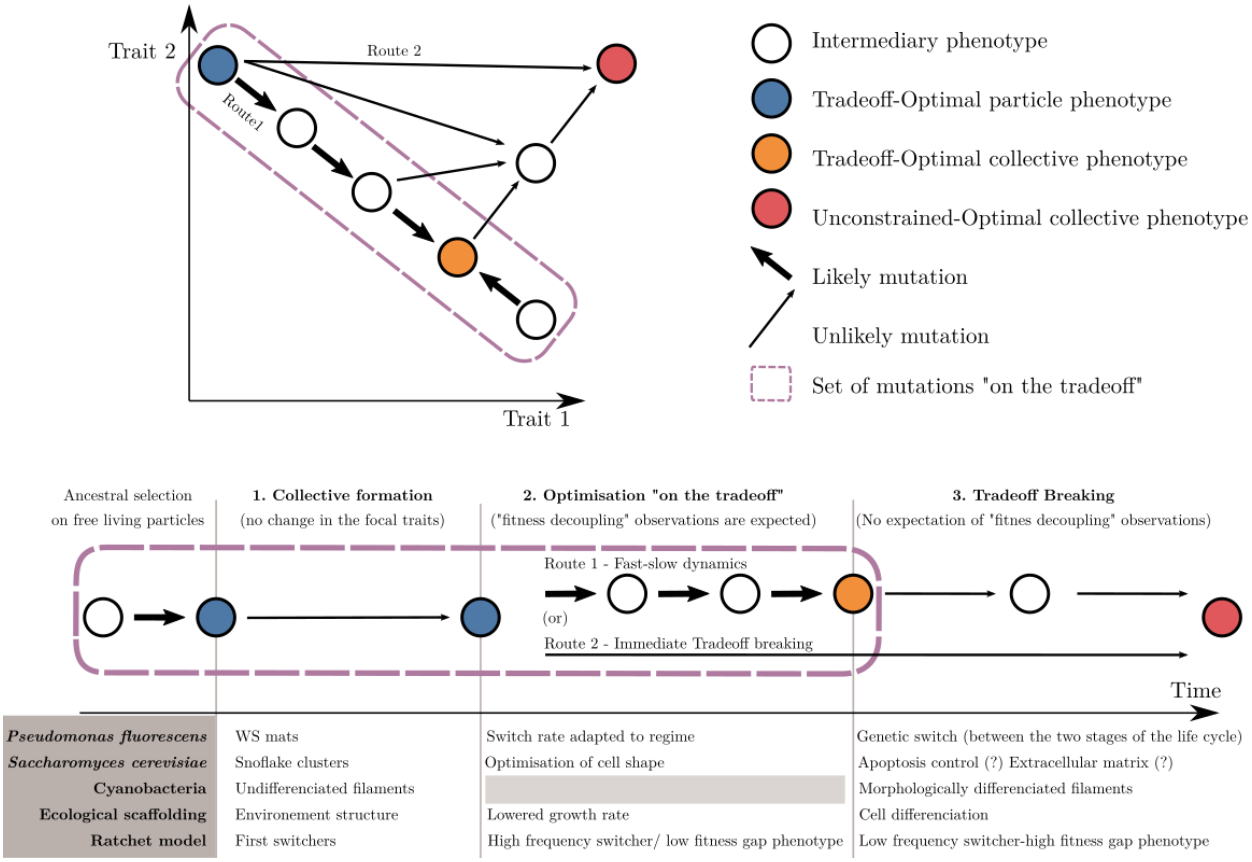

Figure 8 ***An adaptive scenario for ETIs as a consequence of the trait-based approach****. 1. Collective formation of particles occurs by an event that does not change the focal traits. 2. Optimisation "on the tradeoff", where the traits are selected within the constraints passed down from the ancestral organism. 3. Tradeoff breaking, where mutations that are not bound by the ancestral constraints enable tradeoff breaking. Fitness decoupling observations are expected in the second phase but not in the third. Note that the second phase might be shortened or even bypassed depending on the mutational path (this second route "immediate tradeoff breaking" contrasts with the previously described first route "fast-slow dynamics"). This framework can be used to interpret a diversity of*

bioRxiv preprint doi: https://doi.org/10.1101/2021.09.01.458526; this version posted March 1, 2022. The copyright holder for this preprint (which was not certified by peer review) is the author/funder, who has granted bioRxiv a license to display the preprint in perpetuity. It is made available under aCC-BY 4.0 International license.

experimental and mathematical model systems as shown with the examples. P. fluorescens from Hammerschmidt et al., 2014, , S. cerevisiae from Ratcliff et al., 2015, Ecological scaffolding from Black et al., 2020, and Ratchet model from Libby et al., 2016.

The trait-based approach we have described so far delineates an adaptive scenario for an ETI. This scenario is divided into several phases. First, formation of collectives; second, an optimisation within the constraints of the ancestral tradeoff (note that this phase is optional and might be shortened or bypassed depending on the biological system); and third, a tradeoff-breaking phase. In this section, we recast this scenario in the broader context of ETIs and discuss its relevance as a marker of individuality.

Before an ETI starts, the unicellular ancestors have been selected for traits that optimise growth rate in a unicellular environment under the constraints of their genetic constitution ("Tradeoff-Optimal particle phenotype"; blue disk in Figure 8). Then, a mutation (e.g., loss of the transcription factor ACE2, resulting in snowflake-shaped yeast clusters, Ratcliff et al., 2015), a plastic change in phenotype (e.g., filament formation under low population densities in cyanobacteria, Tang et al., 2021), a change in the structure of the environment (as in the ecological scaffolding model for the origin of multicellularity, Black et al., 2020) or even a combination of several factors ("wrinkly spreader" (WS) mats arising by mutation and ecological scaffolding, Hammerschmidt et al., 2014) promote the formation of collectives (Figure 8). Multicellular collectives define a new environment where the optimal trait values are potentially different. We assume here that this change is abrupt and not accompanied by the immediate disappearance of the underlying constraints that bear upon the cell traits, particularly tradeoffs, due to the rest of their genetic machinery. Collective formation is the first phase of our scenario and is often the first phase of any descriptions of an ETI (Bourke, 2011; van Gestel & Tarnita, 2017; Rose & Hammerschmidt, 2021). This has been studied in detail by Tarnita et al. (2013), particularly in the context of competition with the unicellular ancestor. In contrast, our model focuses on what happens after the initial formation of collectives.

In a second phase, we expect changes in traits to occur due to low-hanging fruit mutations, which remain constrained by the ancestral tradeoffs. We call this phase "optimisation on the tradeoff," and it leads the system towards an optimal phenotype for the within-collective environment ("Tradeoff-Optimal collective phenotype", orange disk in Figure 8). We observe trait optimisation on the tradeoff in all our example model systems (Figure 8), except for cyanobacteria. Here, in contrast to the other empirical examples, we do not follow an ETI in progress but one that happened in the evolutionary past so that phase two cannot be observed (anymore) in the known species of today. During this phase in our scenario, fitness decoupling might be observed. For this to occur, the system must meet a few assumptions we made in the previous section: namely, that fitness is a continuous function of traits, and that the ancestral traits are initially optimal for the single-cell environment—and, thus, optimal for counterfactual fitness—but not optimal for the within-collective environment. When these assumptions are met and that selection drives the system towards better trait values (within constraints) for this new within-collective environment, counterfactual fitness will necessarily decrease while collective fitness will necessarily increase (from the blue to the orange disk in Figure 8). If this set of assumptions is violated, nothing can be said about the relationship between counterfactual and collective fitness.

The third phase entails changes in phenotype that lie outside the constraints of the ancestral particles. These are driven by selection of the system towards new, previously unreachable trait values (red disk in Figure 8; "unconstrained optimal collective"). We refer to this third phase as the tradeoff-breaking phase (see Figure 8 for adaptations in our example model systems). During this phase, particle fitness—whether counterfactual (f_2) or

bioRxiv preprint doi: https://doi.org/10.1101/2021.09.01.458526; this version posted March 1, 2022. The copyright holder for this preprint (which was not certified by peer review) is the author/funder, who has granted bioRxiv a license to display the preprint in perpetuity. It is made available under aCC-BY 4.0 International license.

within collectives (f_1)—does not necessarily continue to decrease, even if the conditions for fitness decoupling observations outlined earlier are fulfilled. This is so because the new trait values are in the region of the trait space that was not reachable by the ancestor. In consequence, there is no particular theoretical or biological reason to expect that they would have been suboptimal and selected against, had the ancestor been endowed with such trait values.

If we assume that tradeoff-breaking changes are less likely than the low-hanging fruit mutations constrained by a tradeoff, we statistically expect them to occur predominantly after the second phase, resulting in a "fast-slow dynamic" (route 1 in Figure 8). This route is the focus of the present article. However, while we do not develop this in detail here, depending on the biological system, the second phase might be short if tradeoff-breaking changes are the first to occur. This possibility is particularly relevant for experimental studies. A short second phase implies that it could easily be missed by experimenters. Another possibility is that the second phase is missing entirely (route 2 in Figure 8).

Yet another possibility not studied in this article is that tradeoff-breaking-like observations could be made immediately after collective formation leading to the spontaneous emergence of properties that also confer the collective-living benefits. Thus, tradeoff-breaking dynamics (whether following route 1 or route 2 in Figure 8) could be driven entirely from the phenotypic plasticity of particles, without the need for mutation. For instance, in clonal collectives, one could imagine that phenotypic heterogeneity leads to a primordial form of division of labour (Ispolatov et al., 2012; Ulrich et al., 2018; van Gestel & Tarnita, 2017); van Gestel & Tarnita, 2017 for details). In this "plasticity first" scenario, the different phenotypic states would already be part of the genetic repertoire of the unicellular ancestor.

Our main objective in advocating this trait-based approach is to offer a consistent framework for interpreting models, empirical observation and evolutionary experiments of ETIs, which can accommodate the apparent fitness decoupling observations in addition to the tradeoff-breaking ones without referring to the export-of-fitness metaphor. Provided this empirical objective, it is legitimate to ask to what extent the tradeoff-breaking scenario is representative of ETIs and can be used as a marker that an ETI is underway or has occured. First, one must recognise that tradeoff-breaking might occur outside ETIs. For instance, tradeoff-breaking and, more generally, "constraints breaking" are already considered key events in the evolution of body plans and are expected to be a widespread mechanism for the emergence of novelties (see Galis & Metz, 2007; de Vos et al., 2015). Thus, a tradeoff-breaking event in and of itself cannot be used as a marker of an ETI. However, considering a trait in the context where collectives are formed and maintained (phases 1 and 2) and establishing how those collectives change and potentially overcome the constraints that historically bear on particles (phase 3) offers a good empirical handle to study ETIs. Conversely, the lack of any tradeoff-breaking observation in an empirical system could be used as an indication that the transition is still in its early stages.

Discussion: Beyond fitness decoupling

Fitness-centred approaches to ETIs have been influenced by the concept of fitness-decoupling between lower-level particles and higher-level collectives. In this view, the fitnesses of particles and collectives are initially proportional to one another but diverge as an ETI occurs—particle fitness decreases while collective fitness increases. This interpretation comes with some inconveniences. First, fitness is notoriously difficult to define and measure. This, in turn, makes fitness comparisons across levels difficult. Second, fitness values in and of themselves do not provide a mechanistic model of the system. Progress in understanding ETIs relies on our ability

bioRxiv preprint doi: https://doi.org/10.1101/2021.09.01.458526; this version posted March 1, 2022. The copyright holder for this preprint (which was not certified by peer review) is the author/funder, who has granted bioRxiv a license to display the preprint in perpetuity. It is made available under aCC-BY 4.0 International license.

to circumvent limitations inherent in the currency of fitness. We suggest that, to study ETIs, focusing on traits and tradeoffs between traits, rather than focusing on fitness, is both more parsimonious and practically achievable. Finally, we propose that a general marker of ETIs to use in lieu of fitness decoupling is the emergence of rare tradeoff-breaking mutations.

Our first main finding is a new formal argument cementing the position that decoupling between commensurable measures of fitness is impossible. Starting from the recognition that fitness is a concept difficult to define consistently (Abrams, 2012; Ariew & Lewontin, 2004; Doulcier et al., 2020), the problem is magnified when the entities to be compared belong to different levels of organisation. As we discuss in Section 1 (and Box 1), experimentally comparing fitness in such cases would require being able to measure the growth rates in the same environment at different levels of organisation, which proves challenging. Even if such a comparison could be made, fitness measures at different levels of the same biological substrate necessarily lead to the same outcome at any level. We show this point formally in Section 2. In particular, commensurability is assured by taking care to use the same set of events (same reference environment and same timescales) for both measures. Once this is ensured, fitness decoupling is not observed. Thus, our analysis reveals that fitness-decoupling observations result from incommensurable fitness measurements. We formally confirm the analysis provided by Bourrat (2015a,b; see also Black et al., 2020) who qualifies such observations as artefacts of descriptions. This contradicts the idea that they stem from an export-of-fitness (see Michod et al., 2003; Michod, 2005; Okasha, 2006, 2009; Folse & Roughgarden, 2010).

Our second main finding is that a fitness decoupling observation is not a reliable marker that an ETI is occurring and cannot explain the emergence of trait values outside the scope of the particles/proto-collective tradeoffs. Instead, we propose a tradeoff-breaking model, which produces tradeoff-breaking observations and is more general. In Section 3, we clarify the conditions under which a fitness-decoupling observation (between incommensurable fitness measures) could, in principle, be made—using a simple tradeoff model between traits values, we find that one condition is that the optimal trait values for counterfactual particle fitness and whole–life cycle fitness are different. In Sections 4 and 5, we show that if the tradeoff is relaxed through the existence of rare tradeoff-breaking mutations, fitness-decoupling observations may not hold for whole evolutionary trajectories. We argue that an evolutionary trajectory can be divided into three phases: a first phase during which collectives are formed, followed by an optional second fast-paced phase during which optimisation "on the tradeoff" occurs, and finally a slower phase driven by rare tradeoff-breakings. Tradeoff-breaking mutations might result in lineages where both counterfactual and whole–life cycle fitnesses are increased compared to the ancestor, contrary to the expectation of the export-of-fitness model. We propose that departures in collective-level entities from ancestral tradeoffs—tradeoff-breaking points—are a mark of a key moment of ETIs and might be used to characterise them. This proposal is compatible with recent models found in the literature on ETIs, namely the ecological scaffolding model (Black et al., 2020; Bourrat, in press; Doulcier et al., 2020) and the ratchet model (Libby et al., 2016; Libby & Ratcliff, 2014) that provide alternative mechanisms for both tradeoffs and tradeoff-breaking observations. Further, we show that it is also compatible with experimental data on cyanobacteria

bioRxiv preprint doi: https://doi.org/10.1101/2021.09.01.458526; this version posted March 1, 2022. The copyright holder for this preprint (which was not certified by peer review) is the author/funder, who has granted bioRxiv a license to display the preprint in perpetuity. It is made available under aCC-BY 4.0 International license.

(Colón-López et al., 1997; Misra & Tuli, 2000; Berman-Frank et al., 2003; Popa et al., 2007; Mohr et al., 2013) and *Pseudomonas fluorescens* (Hammerschmidt et al., 2014; Rose et al., 2020).

Our tradeoff-breaking framework could serve as a spring board to generate new hypotheses. The study of tradeoff-breaking requires estimating changes between the pre-ETI ancestral traits (e.g., unicellular) and post-ETI derived traits. Access to ancestral traits can be gained in multiple ways, depending on the system studied. The first is through phylogenetic reasoning, such as, by reconstructing the sequence of ecological and phenotypic trait evolution during the evolution of cyanobacterial multicellularity (as in Hammerschmidt et al., 2021). The second is by assuming that the ancestral traits are close to the optimal values with respect to the counterfactual particle "outside of the collective." The method described by Shelton and Michod (2020), once separated from the export-of-fitness model, would prove useful here. The third is through direct measurement during experimental evolution studies (Ratcliff et al., 2012; Hammerschmidt et al., 2014; Herron et al., 2019). Additionally, statistical methods to better characterise tradeoff-breaking should be developed.

Fitness-centred approaches to ETIs may have reached their limits. We propose to refocus the problem on tradeoffs between traits, thereby bypassing the difficulties inherent in fitness comparisons. The advantages of this move are multiple and range from allowing better experimental accessibility to producing a more mechanistic theory. The way the collective-level context affects the constraints that link traits together is the linchpin of our framework. In particular, we argue that tradeoff-breaking events represent a mark of significant evolutionary innovations towards individuality at the higher level that might be missed by fitness-centred approaches.

bioRxiv preprint doi: https://doi.org/10.1101/2021.09.01.458526; this version posted March 1, 2022. The copyright holder for this preprint (which was not certified by peer review) is the author/funder, who has granted bioRxiv a license to display the preprint in perpetuity. It is made available under aCC-BY 4.0 International license.

Box 1. Comparing Fitnesses

Determining whether the fitness of an entity is higher or lower than that of another entity requires obtaining commensurate fitness estimates for the two entities. In this box, we consider monomorphic lineages; thus, "individual" or "lineage" fitness can be used interchangeably.

A conventional fitness estimate, is an entity's expected number of offspring after one generation. However, for this estimate to be adequate for the purpose of comparison, the generation time of the entities compared must be the same. If they are not, a different/same number of offspring per generation does not necessarily indicate a different/same fitness value. To see this point, suppose two entities A and B, which double at each generation, such as two strains of bacteria. Everything else being equal, A doubles at a *faster* rate than B because it has a shorter generation time. Over the same absolute period, A will have a higher number of descendants than B, and one could infer that A is fitter than B. Figure B1a and b illustrate the situations, respectively, where a fitness comparison is made based on generational (and, thus, invalid) and absolute times (valid).

A more appropriate measure for the purpose of fitness comparison when generation times differ between the focal entities is the long-term growth rate of the population or the Malthusian parameter. These values are often computed from empirical actuarial tables using population projection models (see Caswell, 1989a), or on the repeated census of the population (e.g., in microbiology).

However, long-term growth rates can only be compared if they are made over the same set of events. Any observation where one entity appears fitter than the other, but for which a different set of events has been used (different timescale or different environment), could in reality be one where there is no difference between the two. In other words, it could be a spurious observation.

To take an example where the two environments, rather than the times over which reproductive outputs are measured, are different, consider two identical plants receiving different quantities of resources. The plant receiving more resources produces more seeds. Yet, this difference in reproductive output cannot lead to the conclusion that these two plants have different fitnesses where "fitness" is associated with natural selection. In our example, because the two plants are initially identical, they necessarily have the same fitness. This situation is depicted in Figure B1c and d. In Figure B1c, the fitnesses are compared in two different environments—and, thus, the comparison is invalid—while in Figure B1d, the comparison is made in the same environment.

In some situations where one wants to make fitness comparisons, the environment presents fluctuations in time. In this case too, to be comparable they must refer to the same set of events. For instance, if A is in environment 1, and B is successively in environment 1 and 2, the two resulting fitness values are not comparable because they do not inform one of the potential outcomes of competition in environment 1, in environment 2, or in a temporal succession of the two. This invalid comparison is represented in Figure B1e. Therefore, a condition for comparison, taking into account environmental change, is that the two organisms follow the same temporal succession of environments, as presented in Figure B1f. Note, crucially, that we assume here that whether an entity is in a given environment is independent of its type. If a dependence of the environment on the type exists, this environment effectively becomes an extended phenotype (Lu & Bourrat, 2018).

bioRxiv preprint doi: https://doi.org/10.1101/2021.09.01.458526; this version posted March 1, 2022. The copyright holder for this preprint (which was not certified by peer review) is the author/funder, who has granted bioRxiv a license to display the preprint in perpetuity. It is made available under aCC-BY 4.0 International license.

If the environmental changes are not deterministic, a weaker condition than the same temporal succession of environments is that the two organisms experience the same distribution of environments and transition probabilities between environments (steady-state) (see Doulcier et al., 2021). This type of scenario is not discussed in the main text (but see Box 3).

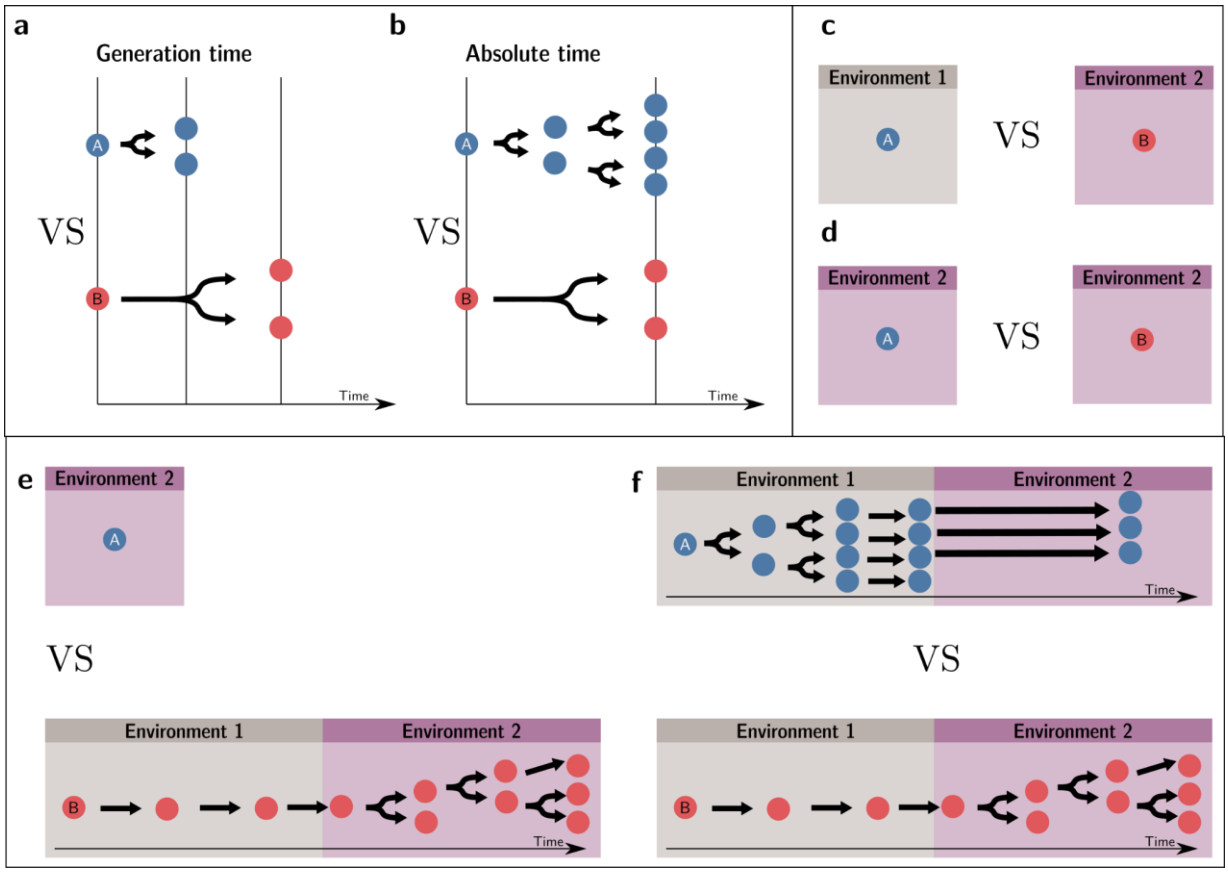

Box 1-figure 1: Valid fitness comparisons require measures over the same set of events (same environment and timescale). *Invalid comparisons: a, c, e,. Valid comparisons: b,d,f.*

bioRxiv preprint doi: https://doi.org/10.1101/2021.09.01.458526; this version posted March 1, 2022. The copyright holder for this preprint (which was not certified by peer review) is the author/funder, who has granted bioRxiv a license to display the preprint in perpetuity. It is made available under aCC-BY 4.0 International license.

Box 2. Ecological Scaffolding and Tradeoff-Breaking

Population structure can lead to the kind of tradeoff presented in Section 3, as seen in the ecological scaffolding scenario for the origin of multicellularity (Black et al., 2020). In this scenario, the population of particles is structured in patches of finite resources with dispersal between patches. The tradeoff evident in this model is between trait values that enhance particle performance within patches and trait values that favor dispersal to new patches. The evolutionary dynamics of two particular traits are studied: particle growth rate and production of soma-like particles that do not disperse themselves but favour the dispersal of the other particles in the patch. In this box, we show how the model of Black et al. (2020) captures the concepts of tradeoff and tradeoff-breaking presented in the main text.

Ecology

We model the dynamics of germ cells (g), soma cells (s), and resources (r) within collectives. Two traits can mutate: the growth rate of germ cells β and the proportion of soma cells that are produced by germ cells q. The ecology within a patch is given by (Equation 3 in Black et al. 2020):

$$\begin{cases} \frac{dg}{dt} = N^{-1}\beta(1-q)r(t)g(t) - g(t) \\ \frac{dr}{dt} = -N^{-1}\beta r(t)g(t) - dr(t)s(t) \\ \frac{ds}{dt} = N^{-1}\beta q r(t)g(t) - s(t) \end{cases},$$

where N is the carrying capacity of a patch and d the rate at which soma cells consume resources. Initial conditions at the beginning of each generation are taken to be: $g(0) = 1$, $r(0) = N$, and $s(0) = 0$. Thus, at the beginning of a collective generation, there is only a single germ cell in the collective. Note that if $q = 0$, there are never any soma cells in the model (for any point t, $s(t) = 0$).

The weight of a patch w in the dispersal phase is given by $w = (1 + \rho s(T))g(T)$, where T is the duration of the growth phase and ρ is the advantage in dispersal conferred by the soma cells. If $\rho = 0$, the soma cells do not affect the dispersal.

Fitnesses

We now recast this model within our framework. The within-collective fitness of cells f_1 (ignoring inter-collective events and density dependence within collectives), is: $f_1 = \left.\frac{d(s(t)+g(t))}{dt}\right|_{s,r,g=(1,N,0)} = \beta$.
The counterfactual fitness f_2 is computed assuming that collectives give rise to free living cells at rate β (and not allowing the production of soma cells); thus, $f_2 = \beta$.

Computing the whole–life cycle fitness F (or f_3) is more challenging since there is (some) density dependence between collectives. However, since collective generations are non-overlapping and collectives only reproduce

bioRxiv preprint doi: https://doi.org/10.1101/2021.09.01.458526; this version posted March 1, 2022. The copyright holder for this preprint (which was not certified by peer review) is the author/funder, who has granted bioRxiv a license to display the preprint in perpetuity. It is made available under aCC-BY 4.0 International license.

once (at the end of their life), the only number that matters, in the long run, is the weight of a patch (the number of dispersing propagules) at the time of dispersal: $F \approx w$.

Figure B2a shows the set of accessible phenotypes when mutations occur on either β or q. From this figure, it is possible to predict what will happen in a hypothetical scenario of sequential mutations on β then q. Starting from point *a*, if only β is able to mutate, we can expect the population to move to *b* (the highest value of F for $q = 0$, while f_2 decreases), optimising on the tradeoff. Note that β plays the same role as θ in Section 3, encoding the linear abscissa of the cells on the tradeoff line. If mutations affecting q become possible once the population reaches *b*, the population is expected to evolve towards *c*, without change in f_2, breaking the previously defined tradeoff. This requires that mutations happen on one trait and then the other. This assumption will be relaxed in the next paragraph by using the same method as in Section 4.

Evolution

Let (q, β) be the vector of traits characterising a phenotype. We compute the evolutionary trajectory using the same Lande-Equation model as in Section 4, namely Eq 3. G is the variance-covariance matrix of mutational effects. In this example, consider that mutational effects on both traits are not correlated ($\rho = 0$ using the notation of the main text), and that the mutational effect variance for β is much higher than for q: $\sigma_\beta = 0.1$ and $\sigma_q = 0.001$. This assumes that most mutations have a higher effect on β than q.

Figure B2b and B2c show a trajectory simulated this way, with initial conditions $(q_0, \beta_0) = (0, 1.8)$, which displays a dynamic akin to the one in Section 4: a fast-paced phase where frequent low-hanging fruit mutations (mainly affecting β) are reached by the population, increasing F (between t_0 and t_1, note that f_2 simultaneously decreases). This fast-paced phase is followed by a slow-paced phasee where an increase in F is only possible through rarer mutations (mainly affecting q) (after t_1, note that f_2 simultaneously increases) and leads to a tradeoff-breaking observation similar to the one described in Section 4.

To summarise, this simple set of hypotheses (initial conditions, rarer mutations on q than on β) lead to a transient fitness-decoupling observation. Notably, this observation does not stem from mutational effects (like in the main text), but from the ecological constraints on β that do not allow F and f_2 to be maximised for the same conditions (purple line in Figure B2a). Tradeoff-breaking is due to rarer mutations on q (as in the main text where rare mutations increase both survival and growth rate).

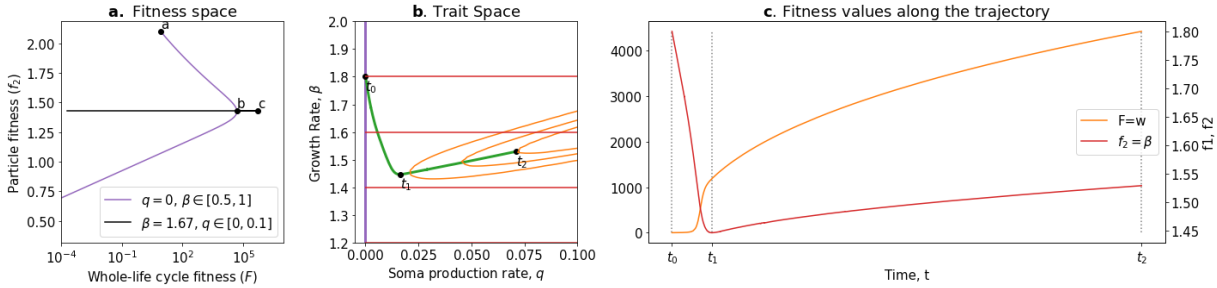

Box 2-figure 1 Tradeoff-breaking in the ecological scaffolding scenario a. *Values of F and f_2 accessible to the organism when $q = 0$ and only β can mutate (purple) and values of F and f_2 accessible to the organism when only q can mutate and β is such that F is maximum for $q = 0$ (black);* ***b.*** *Trait space with isolines of fitness (f_2 in red, F in orange), with an example of evolutionary trajectory in green (ancestral tradeoff represented in purple).* ***c.*** *f_2 and F values along the example evolutionary trajectory. The times marked by vertical lines in* ***c.***

bioRxiv preprint doi: https://doi.org/10.1101/2021.09.01.458526; this version posted March 1, 2022. The copyright holder for this preprint (which was not certified by peer review) is the author/funder, who has granted bioRxiv a license to display the preprint in perpetuity. It is made available under aCC-BY 4.0 International license.

correspond to the dots in ***b****. Note that* F *and* f_2 *have opposed dynamics from* t_0 *to* t_1 *(fitness decoupling observation) and both increase from* t_1 *to* t_2*. Rare mutations on* q *allow breaking away from the ancestral tradeoff line (tradeoff-breaking observation). Parameters:* $N = 1e+06$, *T=30d=0*$\rho = 0.01$, $\sigma_\beta = 0.1$, $\sigma_q = 0.001$.

bioRxiv preprint doi: https://doi.org/10.1101/2021.09.01.458526; this version posted March 1, 2022. The copyright holder for this preprint (which was not certified by peer review) is the author/funder, who has granted bioRxiv a license to display the preprint in perpetuity. It is made available under aCC-BY 4.0 International license.

Box 3. Ratcheting and Tradeoff-Breaking

Tradeoff-breaking mutations are equivalent to rare mutations that change the set of accessible phenotypes. Libby et al. (2016) propose a mechanism of ratcheting mutations that stabilises multicellularity by constraining evolutionary reversion towards unicellularity. They consider a nascent multicellular organism that switches between a multicellular G and unicellular state I, growing in an environment alternating between two states, one favoring the multicellular life cycle (E_G) and the other favoring unicellular life cycle (E_I). Two types of ratcheting can occur: first, mutations that improve the fitness within the multicellular type that come at a cost to the free-living type (reducing the fitness of revertants) and, second, a type of ratcheting mutation that decreases the probability that a mutation results in reversion. In the following, we show how the slowest of type 1 or type 2 ratcheting fits as a tradeoff-breaking mechanism, as presented in the main text.

The population dynamics of both types G_t and I_t in an environment that fluctuates between E_G and E_I after a fixed number of generations in each (n_g and n_i respectively) is given by Equation 2.3 from Libby et al. (2016):

$$\begin{pmatrix} G_{t+n_g+n_i} \\ I_{t_{ng}+n_i} \end{pmatrix} = \begin{pmatrix} (1-c_i)(1-p)+1 & p \\ (1-c_i)p & 1+(1-p) \end{pmatrix}^{n_i} \begin{pmatrix} 1+(1-p) & (1-c_g)p \\ p & (1-c_g)(1-p)+1 \end{pmatrix}^{n_g} \begin{pmatrix} G_t \\ I_t \end{pmatrix}$$
$$= \mathbf{A}_I^{n_i} \mathbf{A}_G^{n_g} \begin{pmatrix} G_t \\ I_t \end{pmatrix} = \mathbf{A} \begin{pmatrix} G_t \\ I_t \end{pmatrix}$$

where p is the probability for cells to switch from one type to the other, and $c_g, c_i > 0$ are the fitness differences between G and I cells in E_G and E_I environmental states, respectively. In the following, we fix $c_g = 0.1$ and the traits that can mutate are p and the fitness gap $\Delta c = c_g - c_i$.

We now recast this model within our framework. The whole–life cycle fitness of the organism F is the log of the the dominant eigenvalue of the matrix $\mathbf{A}$, the counterfactual fitness f_2 is the fitness of the organisms if they would always be in the E_I environment ($n_g = 0$)—that is, the log of the dominant eigenvalue of $\mathbf{A}_I$. Conversely, the within-collective fitness f_1 is the fitness of the cells if they would constantly be in the E_G environment—thus, the log of the dominant eigenvalue of $\mathbf{A}_G$.

Let $(\Delta c, p)$ be the trait vector characterizing a phenotype, and let us model evolution using the equation from Section 4 Eq 3, considering that mutations affecting p (ratcheting type 2) are more frequent than mutations affecting Δc (ratcheting type 1): $\sigma_{\Delta c} = 10^{-4}, \sigma_p = 0.2$. Initial traits values are $\Delta c = 0$ and $p = 10^{-5}$ (no fitness gap and very rare switch).

Figure B3b and B3c shows the result of the simulation. The evolutionary trajectory can be split into three phases: first, a fast-paced phase where the switch probability p increases to 0.2, corresponding to optimisation on the tradeoff (before t_1, note that here p plays the same role as θ in Section 3, giving the linear abscissa of the cells on the tradeoff line); then a slow increase in Δc, corresponding to the slow accumulation of tradeoff-breaking mutations (type 1 ratcheting) leading to a tradeoff-breaking observation (between t_1 and t_2); and, finally, a new decrease in switch probability (type 2 ratcheting), corresponding to an optimisation on the (new) tradeoff (after t_2). The result is an overall increase in the proportion of G-type in the population (Figure B3c).

bioRxiv preprint doi: https://doi.org/10.1101/2021.09.01.458526; this version posted March 1, 2022. The copyright holder for this preprint (which was not certified by peer review) is the author/funder, who has granted bioRxiv a license to display the preprint in perpetuity. It is made available under aCC-BY 4.0 International license.

Note that F always increases along the trajectory. However, f_2 decreases in the first phase and increases in the second and third phases, showing trajectories that the fitness decoupling model cannot easily account for.

To summarise, this simple set of hypotheses (ratcheting type 1 and 2, with mutations for ratcheting 1 being rarer) lead to a fitness-decoupling observation when selection first acts along the switch probability tradeoff (leading to higher switching, and an increase in multicellular types) because the optimal trait values for F and f_2 are different. Then, rarer type 2 ratcheting mutations result in tradeoff-breaking, eventually resulting in a second (relatively fast-paced) optimisation on the switch-probability tradeoff (leading to reduced switching and entrenchment of the multicellular type), which does not result in a fitness-decoupling observation because the optimal trait value for F and f_2 coincide. Note that, here, the tradeoff stems from the ratcheting mechanism and the environment periodically switching between multicellularity or unicell-favoring, rather than the genetic architecture (as in the main text) or population structure (as in Box 2).

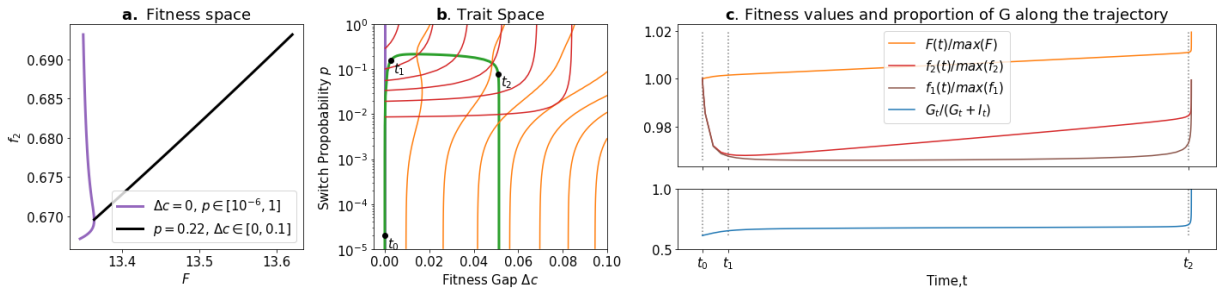

Box 3-figure 1: Ratcheting and Tradeoff-breaking. a*. Values of F and f_2 accessible to organisms when $\Delta c = 0$ and p is free (purple), and when p=0.2 and Δc is free (black).* ***b.*** *Trait space with isolines of fitness (f_2 in red, F in orange) with an example of evolutionary trajectory in green (ancestral tradeoff represented in purple).* ***c.*** *Fitness values for f_1 (in brown), f_2 and F in addition to the stable proportion of G (in blue) along the example evolutionary trajectory. The times marked by vertical lines in* ***c.*** *correspond to the dots in* ***b.*** *Note that F and f_2 have opposed dynamics from t_0 to t_1 (fitness decoupling observation), and both increase after t_1. Rare mutations on Δc allow to break-away from the ancestral tradeoff line (tradeoff-breaking observation) after t_1. Parameters: $c_g = 0.1$, $\sigma_{\Delta c} = 10^{-4}$, $\sigma_p = 0.2$.*

bioRxiv preprint doi: https://doi.org/10.1101/2021.09.01.458526; this version posted March 1, 2022. The copyright holder for this preprint (which was not certified by peer review) is the author/funder, who has granted bioRxiv a license to display the preprint in perpetuity. It is made available under aCC-BY 4.0 International license.

Glossary

-*Particles* or *cells:* The lower-level entities of a two-level biological system.
-*Collectives* or *multicells:* The higher-level entities of a two-level biological system.
-*Evolutionary transition in individuality* (ETI): Evolutionary process during which collective-level entities become evolutionary individuals and are able to participate in the process of evolution by natural selection "in their own right".
-*Fitness*: The expected average exponential growth rate of a given type of individual (i.e., individual sharing the same traits) in a given steady-state reference environment.
-*Fitness-decoupling observation*: The observation that the fitness of particles decreases while the fitness of collectives increases. Used in the literature as a probable hallmark of an ETI.
-*Within-collective particle fitness:* The fitness of a particle within the collective environnement, ignoring collective-level events (for instance because they happen at a longer time scale). Noted f_1 in the main text.
- *Counterfactual particle fitness:* The fitness of a hypothetical particle with the same traits as the actual particle that would live in a non-collective reference environment.. There is no unique way to define the counterfactual reference environment. Noted f_2 in the main text.
- *Whole–life cycle particle fitness:* The fitness of a particle computed over a reference environment that includes the whole life cycle of collectives (including collective birth–death events). Mathematically equal to the collective-level fitness if the collective stage distribution reaches a steady state (i.e., collectives do not keep getting bigger or smaller) as proven in Section 2. Noted f_3 in the manuscript.
- *Export-of-fitness model:* A model used to explain *fitness-decoupling observations* by a "transfer of fitness" from the particle level to the collective level during ETIs.
- *Tradeoff model*: An alternative model to the *export-of-fitness model* used to explain *fitness-decoupling observations* by invoking ecological or genetic constraints on the values of traits that contribute to *counterfactual* and *whole–life cycle fitness* during an ETI.
- *Tradeoff-breaking observation:* The observation that some lineages do not seem to conform to the *fitness-decoupling observation* during an ETI—they show an increase of both counterfactual or within-collective fitness and collective fitness.
- *Tradeoff-breaking model:* A model where the evolutionary trajectories follow constraints that come from the unicellular ancestors (tradeoff) and that include rare mutations that are not submitted to the same constraints (tradeoff-breaking). This model can account for both fitness-decoupling and tradeoff-breaking observations during ETIs.

References

bioRxiv preprint doi: https://doi.org/10.1101/2021.09.01.458526; this version posted March 1, 2022. The copyright holder for this preprint (which was not certified by peer review) is the author/funder, who has granted bioRxiv a license to display the preprint in perpetuity. It is made available under aCC-BY 4.0 International license.

Abrams, M. (2012). Measured, Modeled, and Causal Conceptions of Fitness. *Frontiers in Genetics*, *3*, 196.

Amdam, G. V., & Page, R. E. (2010). The developmental genetics and physiology of honeybee societies. *Animal Behaviour*, *79*(5), 973–980. https://doi.org/10.1016/j.anbehav.2010.02.007

Ariew, A., & Lewontin, R. C. (2004). The Confusions of Fitness. *The British Journal for the Philosophy of Science*, *55*(2), 347–363.

Berman-Frank, I., Lundgren, P., & Falkowski, P. (2003). Nitrogen fixation and photosynthetic oxygen evolution in cyanobacteria. *Research in Microbiology*, *154*(3), 157–164. https://doi.org/10.1016/S0923-2508(03)00029-9

Bienvenu, F., & Doulcier, G. (2021). *MatPopMod, a Python library for matrix population models*. Zenodo. https://doi.org/10.5281/zenodo.5711709

Black, A. J., Bourrat, P., & Rainey, P. B. (2020). Ecological scaffolding and the evolution of individuality. *Nature Ecology & Evolution*, *4*, 426–436. https://doi.org/10.1038/s41559-019-1086-9

Bouchard, F., & Huneman, P. (2013). *From Groups to Individuals: Evolution and Emerging Individuality*. MIT Press.

Bourke, A. F. (2011). *Principles of social evolution*. Oxford University Press.

Bourrat, P. (2015a). Levels of selection are artefacts of different fitness temporal measures. *Ratio*, *28*(1), 40–50.

Bourrat, P. (2015b). Levels, time and fitness in evolutionary transitions in individuality. *Philosophy & Theory in Biology*, *7*. http://dx.doi.org/10.3998/ptb.6959004.0007.001

Bourrat, P. (2021a). Transitions in evolution: A formal analysis. *Synthese*, *198*(4), 3699–3731. https://doi.org/10.1007/s11229-019-02307-5

Bourrat, P. (2021b). *Facts, Conventions, and the Levels of Selection* (Cambridge University Press). https://www.cambridge.org/core/elements/facts-conventions-and-the-levels-of-selection/8EAF88974A3BE92761217A2EC6AB4634

bioRxiv preprint doi: https://doi.org/10.1101/2021.09.01.458526; this version posted March 1, 2022. The copyright holder for this preprint (which was not certified by peer review) is the author/funder, who has granted bioRxiv a license to display the preprint in perpetuity. It is made available under aCC-BY 4.0 International license.

Bourrat, P. (in press). Evolutionary Transitions in Individuality by Endogenization of Scaffolded Properties. *The British Journal for the Philosophy of Science*, 719118. https://doi.org/10.1086/719118

Buss, L. W. (1987). *The Evolution of Individuality*. Princeton University Press.

Calcott, B., & Sterelny, K. (2011). *The major transitions in evolution revisited*. MIT Press.

Caswell, H. (1989a). *Matrix Population Models*. Sinauer Associates.

Caswell, H. (1989b). *Matrix population models: Construction, analysis, and interpretation*. Sinauer Associates.

Colón-López, M. S., Sherman, D. M., & Sherman, L. A. (1997). Transcriptional and translational regulation of nitrogenase in light-dark- and continuous-light-grown cultures of the unicellular cyanobacterium Cyanothece sp. Strain ATCC 51142. *Journal of Bacteriology*, *179*(13), 4319–4327. https://doi.org/10.1128/jb.179.13.4319-4327.1997

Conlin, P. L., Kahn, P. C., Beck, T. von, Borin, J. M., Marquez-Zacarias, P., Bozdag, G. O., Kerr, B., & Ratcliff, W. C. (2019, June 26). *Origin and consequences of fitness decoupling during the evolutionary transition to multicellularity*. 2019 Astrobiology Science Conference. https://agu.confex.com/agu/abscicon19/meetingapp.cgi/Paper/482349

Davison, D. R., & Michod, R. E. (2021). Phenotypic Plasticity and Evolutionary Transitions in Individuality. In *Phenotypic Plasticity & Evolution*. CRC Press.

de Vos, M. G. J., Dawid, A., Sunderlikova, V., & Tans, S. J. (2015). Breaking evolutionary constraint with a tradeoff ratchet. *Proceedings of the National Academy of Sciences*, *112*(48), 14906–14911. https://doi.org/10.1073/pnas.1510282112

Doebeli, M., Ispolatov, Y., & Simon, B. (2017). Towards a mechanistic foundation of evolutionary theory. *ELife*, *6*, e23804. https://doi.org/10.7554/eLife.23804

Doulcier, G., Lambert, A., De Monte, S., & Rainey, P. B. (2020). Eco-evolutionary dynamics of nested Darwinian populations and the emergence of community-level heredity. *ELife*, *9*, e53433.

bioRxiv preprint doi: https://doi.org/10.1101/2021.09.01.458526; this version posted March 1, 2022. The copyright holder for this preprint (which was not certified by peer review) is the author/funder, who has granted bioRxiv a license to display the preprint in perpetuity. It is made available under aCC-BY 4.0 International license.

https://doi.org/10.7554/eLife.53433

Doulcier, G., Takacs, P., & Bourrat, P. (2021). Taming fitness: Organism-environment interdependencies preclude long-term fitness forecasting. *BioEssays*, *43*(1), 2000157. https://doi.org/10.1002/bies.202000157

Fisher, R. A. (1930). *The genetical theory of natural selection*. Oxford University Press.

Folse, H. J., & Roughgarden, J. (2010). What is an individual organism? A multilevel selection perspective. *The Quarterly Review of Biology*, *85*, 447–472.

Galis, F., & Metz, J. A. J. (2007). Evolutionary novelties: The making and breaking of pleiotropic constraints. *Integrative and Comparative Biology*, *47*(3), 409–419. https://doi.org/10.1093/icb/icm081

Hammerschmidt, K., Landan, G., Domingues Kümmel Tria, F., Alcorta, J., & Dagan, T. (2021). The order of trait emergence in the evolution of cyanobacterial multicellularity. *Genome Biology and Evolution*, *13*(2), evaa249. https://doi.org/10.1093/gbe/evaa249

Hammerschmidt, K., Rose, C. J., Kerr, B., & Rainey, P. B. (2014). Life cycles, fitness decoupling and the evolution of multicellularity. *Nature*, *515*(7525), 75–79.

Hanschen, E. R., Davison, D. R., Grochau-Wright, Z. I., & Michod, R. E. (2017). Evolution of Individuality: A Case Study in the Volvocine Green Algae. *Philosophy, Theory, and Practice in Biology*, *9*(20171201). https://doi.org/10.3998/ptb.6959004.0009.003

Hanschen, E. R., Shelton, D. E., & Michod, R. E. (2015a). Evolutionary Transitions in Individuality and Recent Models of Multicellularity. In I. Ruiz-Trillo & A. M. Nedelcu (Eds.), *Evolutionary Transitions to Multicellular Life* (Vol. 2, pp. 165–188). Springer Netherlands. https://doi.org/10.1007/978-94-017-9642-2_9

Hanschen, E. R., Shelton, D. E., & Michod, R. E. (2015b). Evolutionary Transitions in Individuality and Recent Models of Multicellularity. In I. Ruiz-Trillo & A. M. Nedelcu (Eds.), *Evolutionary Transitions*

bioRxiv preprint doi: https://doi.org/10.1101/2021.09.01.458526; this version posted March 1, 2022. The copyright holder for this preprint (which was not certified by peer review) is the author/funder, who has granted bioRxiv a license to display the preprint in perpetuity. It is made available under aCC-BY 4.0 International license.

to Multicellular Life (Vol. 2, pp. 165–188). Springer Netherlands. https://doi.org/10.1007/978-94-017-9642-2_9

Herron, M. D., Borin, J. M., Boswell, J. C., Walker, J., Chen, I.-C. K., Knox, C. A., Boyd, M., Rosenzweig, F., & Ratcliff, W. C. (2019). De novo origins of multicellularity in response to predation. *Scientific Reports*, *9*(1), 2328. https://doi.org/10.1038/s41598-019-39558-8

Ispolatov, I., Ackermann, M., & Doebeli, M. (2012). Division of labour and the evolution of multicellularity. *Proceedings of the Royal Society B: Biological Sciences*, *279*(1734), 1768–1776. https://doi.org/10.1098/rspb.2011.1999

Jablonka, E. (1994). Inheritance systems and the evolution of new levels of individuality. *Journal of Theoretical Biology*, *170*, 301–309.

Lenski, R. E., Rose, M. R., Simpson, S. C., & Tadler, S. C. (1991). Long-Term Experimental Evolution in Escherichia coli. I. Adaptation and Divergence During 2,000 Generations. *The American Naturalist*, *138*(6), 1315–1341.

Leslie, P. H. (1945). On the Use of Matrices in Certain Population Mathematics. *Biometrika*, *33*(3), 183–212. https://doi.org/10.2307/2332297

Libby, E., Conlin, P. L., Kerr, B., & Ratcliff, W. C. (2016). Stabilizing multicellularity through ratcheting. *Philosophical Transactions of the Royal Society B: Biological Sciences*, *371*(1701), 20150444. https://doi.org/10.1098/rstb.2015.0444

Libby, E., & Ratcliff, W. C. (2014). Ratcheting the evolution of multicellularity. *Science*, *346*(6208), 426–427. https://doi.org/10.1126/science.1262053

Maynard Smith, J., & Szathmáry, E. (1995). *The Major Transitions in Evolution*. W.H. Freeman.

Merlo, L. M. F., Pepper, J. W., Reid, B. J., & Maley, C. C. (2006). Cancer as an evolutionary and ecological process. *Nature Reviews Cancer*, *6*(12), 924–935. https://doi.org/10.1038/nrc2013

bioRxiv preprint doi: https://doi.org/10.1101/2021.09.01.458526; this version posted March 1, 2022. The copyright holder for this preprint (which was not certified by peer review) is the author/funder, who has granted bioRxiv a license to display the preprint in perpetuity. It is made available under aCC-BY 4.0 International license.

Metz, J. A. J., Nisbet, R. M., & Geritz, S. A. H. (1992). How should we define 'fitness' for general ecological scenarios? *Trends in Ecology & Evolution*, *7*(6), 198–202. https://doi.org/10.1016/0169-5347(92)90073-K

Michod, R. E. (1999). *Darwinian dynamics*. Princeton University Press.

Michod, R. E. (2005). On the transfer of fitness from the cell to the multicellular organism. *Biology and Philosophy*, *20*(5), 967–987.

Michod, R. E., & Nedelcu, A. M. (2003). On the reorganization of fitness during evolutionary transitions in individuality. *Integrative and Comparative Biology*, *43*(1), 64–73. https://doi.org/10.1093/icb/43.1.64

Michod, R. E., Nedelcu, A. M., & Roze, D. (2003). Cooperation and conflict in the evolution of individuality: IV. Conflict mediation and evolvability in Volvox carteri. *BioSystems*, *69*(2–3), 95–114.

Michod, R. E., & Roze, D. (1999). Cooperation and Conflict in the Evolution of Individuality. III. Transitions in the Unit of Fitness. In C. L. Nehaniv (Ed.), *Mathematical and Computational Biology: Computational Morphogenesis, Hierarchical Complexity and Digital Evolution* (pp. 47–92). American Mathematical Society.

Misra, H. S., & Tuli, R. (2000). Differential expression of photosynthesis and nitrogen fixation genes in the cyanobacterium Plectonema boryanum. *Plant Physiology*, *122*(3), 731–736. https://doi.org/10.1104/pp.122.3.731

Mohr, W., Vagner, T., Kuypers, M. M. M., Ackermann, M., & LaRoche, J. (2013). Resolution of conflicting signals at the single-cell level in the regulation of cyanobacterial photosynthesis and nitrogen fixation. *PLoS ONE*, *8*(6), e66060. https://doi.org/10.1371/journal.pone.0066060

Okasha, S. (2006). *Evolution and the levels of selection* (Vol. 16). Clarendon Press.

Okasha, S. (2009). Individuals, groups, fitness and utility: Multi-level selection meets social choice theory. *Biology & Philosophy*, *24*(5), 561–584. https://doi.org/10.1007/s10539-009-9154-1

bioRxiv preprint doi: https://doi.org/10.1101/2021.09.01.458526; this version posted March 1, 2022. The copyright holder for this preprint (which was not certified by peer review) is the author/funder, who has granted bioRxiv a license to display the preprint in perpetuity. It is made available under aCC-BY 4.0 International license.

Pence, C. H., & Ramsey, G. (2013). A New Foundation for the Propensity Interpretation of Fitness. *The British Journal for the Philosophy of Science*, *64*(4), 851–881. https://doi.org/10.1093/bjps/axs037

Pichugin, Y. (2015). *Theoretical investigation into the origins of multicellularity: A thesis presented in partial fulfilment of the requirements for the degree of PhD in Theoretical Biology at Massey University, Albany, New Zealand* [Thesis, Massey University]. https://mro.massey.ac.nz/handle/10179/11074

Pichugin, Y., Peña, J., Rainey, P. B., & Traulsen, A. (2017). Fragmentation modes and the evolution of life cycles. *PLOS Computational Biology*, *13*(11), e1005860. https://doi.org/10.1371/journal.pcbi.1005860

Popa, R., Weber, P. K., Pett-Ridge, J., Finzi, J. A., Fallon, S. J., Hutcheon, I. D., Nealson, K. H., & Capone, D. G. (2007). Carbon and nitrogen fixation and metabolite exchange in and between individual cells of Anabaena oscillarioides. *The ISME Journal*, *1*(4), 354–360. https://doi.org/10.1038/ismej.2007.44

Rainey, P. B., & Kerr, B. (2010). Cheats as first propagules: A new hypothesis for the evolution of individuality during the transition from single cells to multicellularity. *BioEssays*, *32*(10), 872–880. https://doi.org/10.1002/bies.201000039

Ratcliff, W. C., Denison, R. F., Borrello, M., & Travisano, M. (2012). Experimental evolution of multicellularity. *Proceedings of the National Academy of Sciences*, *109*(5), 1595–1600. https://doi.org/10.1073/pnas.1115323109

Rose, C. J., Hammerschmidt, K., Pichugin, Y., & Rainey, P. B. (2018). *Meta-population structure and the evolutionary transition to multicellularity* [Data set]. https://doi.org/10.1101/407163

Rose, C. J., Hammerschmidt, K., Pichugin, Y., & Rainey, P. B. (2020). Meta-population structure and the evolutionary transition to multicellularity. *Ecology Letters*, *23*(9), 1380–1390. https://doi.org/10.1111/ele.13570

Shelton, D. E., & Michod, R. E. (2010). Philosophical foundations for the hierarchy of life. *Biology &*

bioRxiv preprint doi: https://doi.org/10.1101/2021.09.01.458526; this version posted March 1, 2022. The copyright holder for this preprint (which was not certified by peer review) is the author/funder, who has granted bioRxiv a license to display the preprint in perpetuity. It is made available under aCC-BY 4.0 International license.

Philosophy, *25*(3), 391–403. https://doi.org/10.1007/s10539-009-9160-3

Shelton, D. E., & Michod, R. E. (2014). Group Selection and Group Adaptation During a Major Evolutionary Transition: Insights from the Evolution of Multicellularity in the Volvocine Algae. *Biological Theory*, *9*(4), 452–469.

Shelton, D. E., & Michod, R. E. (2020). Group and individual selection during evolutionary transitions in individuality: Meanings and partitions. *Philosophical Transactions of the Royal Society B: Biological Sciences*, *375*(1797), 20190364. https://doi.org/10.1098/rstb.2019.0364

Tang, S., Pichugin, Y., & Hammerschmidt, K. (2021). *Phenotypic plasticity, life cycles, and the evolutionary transition to multicellularity* (p. 2021.09.29.462355). bioRxiv. https://doi.org/10.1101/2021.09.29.462355

Tarnita, C. E., Taubes, C. H., & Nowak, M. A. (2013). Evolutionary construction by staying together and coming together. *Journal of Theoretical Biology*, *320*, 10–22. https://doi.org/10.1016/j.jtbi.2012.11.022

Ulrich, Y., Saragosti, J., Tokita, C. K., Tarnita, C. E., & Kronauer, D. J. C. (2018). Fitness benefits and emergent division of labour at the onset of group living. *Nature*, *560*(7720), 635–638. https://doi.org/10.1038/s41586-018-0422-6

van Gestel, J., & Tarnita, C. E. (2017). On the origin of biological construction, with a focus on multicellularity. *Proceedings of the National Academy of Sciences*, 201704631. https://doi.org/10.1073/pnas.1704631114

Werren, J. H. (2011). Selfish genetic elements, genetic conflict, and evolutionary innovation. *Proceedings of the National Academy of Sciences*, *108*(Supplement 2), 10863–10870. https://doi.org/10.1073/pnas.1102343108

West, S. A., Fisher, R. M., Gardner, A., & Kiers, E. T. (2015). Major evolutionary transitions in individuality.

bioRxiv preprint doi: https://doi.org/10.1101/2021.09.01.458526; this version posted March 1, 2022. The copyright holder for this preprint (which was not certified by peer review) is the author/funder, who has granted bioRxiv a license to display the preprint in perpetuity. It is made available under aCC-BY 4.0 International license.

Proceedings of the National Academy of Sciences of the United States of America, *112*(33), 10112–10119.

Wiser, M. J., & Lenski, R. E. (2015). A Comparison of Methods to Measure Fitness in Escherichia coli. *PLOS ONE*, *10*(5), e0126210. https://doi.org/10.1371/journal.pone.0126210

Wiser, M. J., Ribeck, N., & Lenski, R. E. (2013). Long-Term Dynamics of Adaptation in Asexual Populations. *Science*, *342*(6164), 1364–1367. https://doi.org/10.1126/science.1243357